Galactic & Extragalactic Foregrounds

Ad: CHIME and the 26 m Telescope

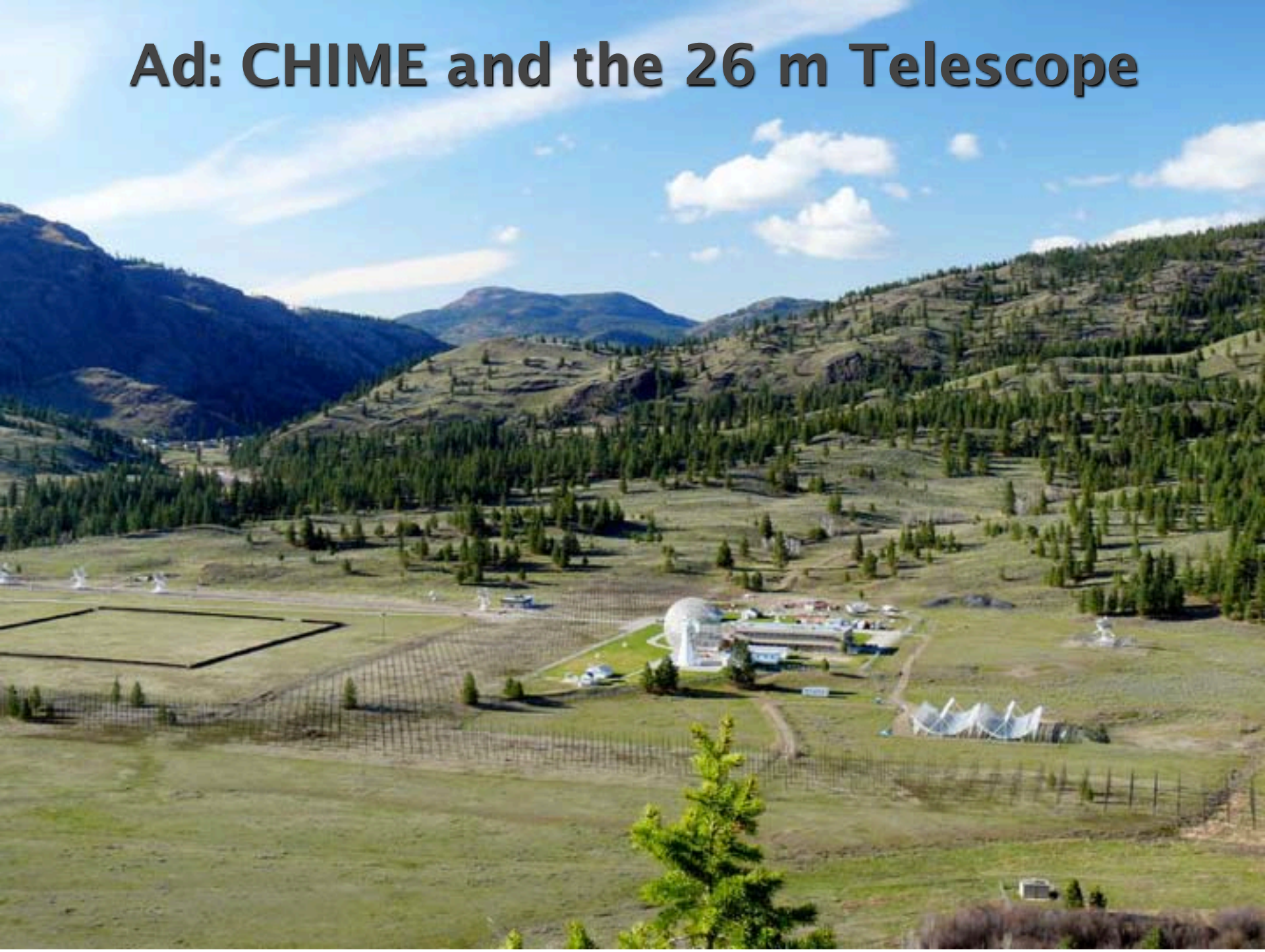

Talk Outline

Galactic foregrounds in CMB studies - unpolarized

Galactic foregrounds in CMB studies - polarized

Extragalactic foregrounds as science -
Sunyaev-Zel'dovich effect as a gas probe

Galactic foregrounds in 21 cm studies -
the "mother of all" foreground problems

Galactic Foregrounds – Unpolarized

Galactic Foreground Spectra

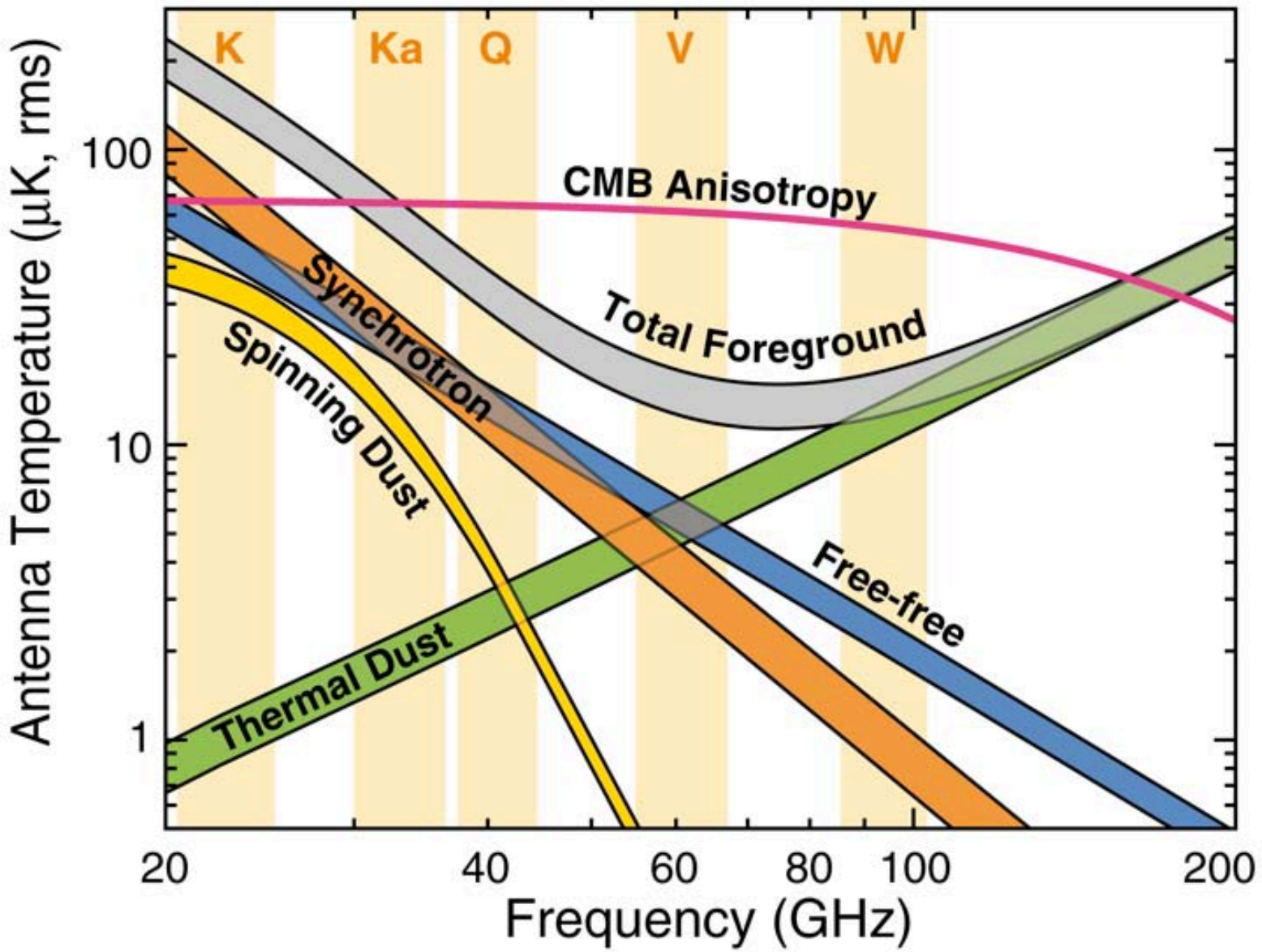

Synchrotron Emission (Haslam 408 MHz)

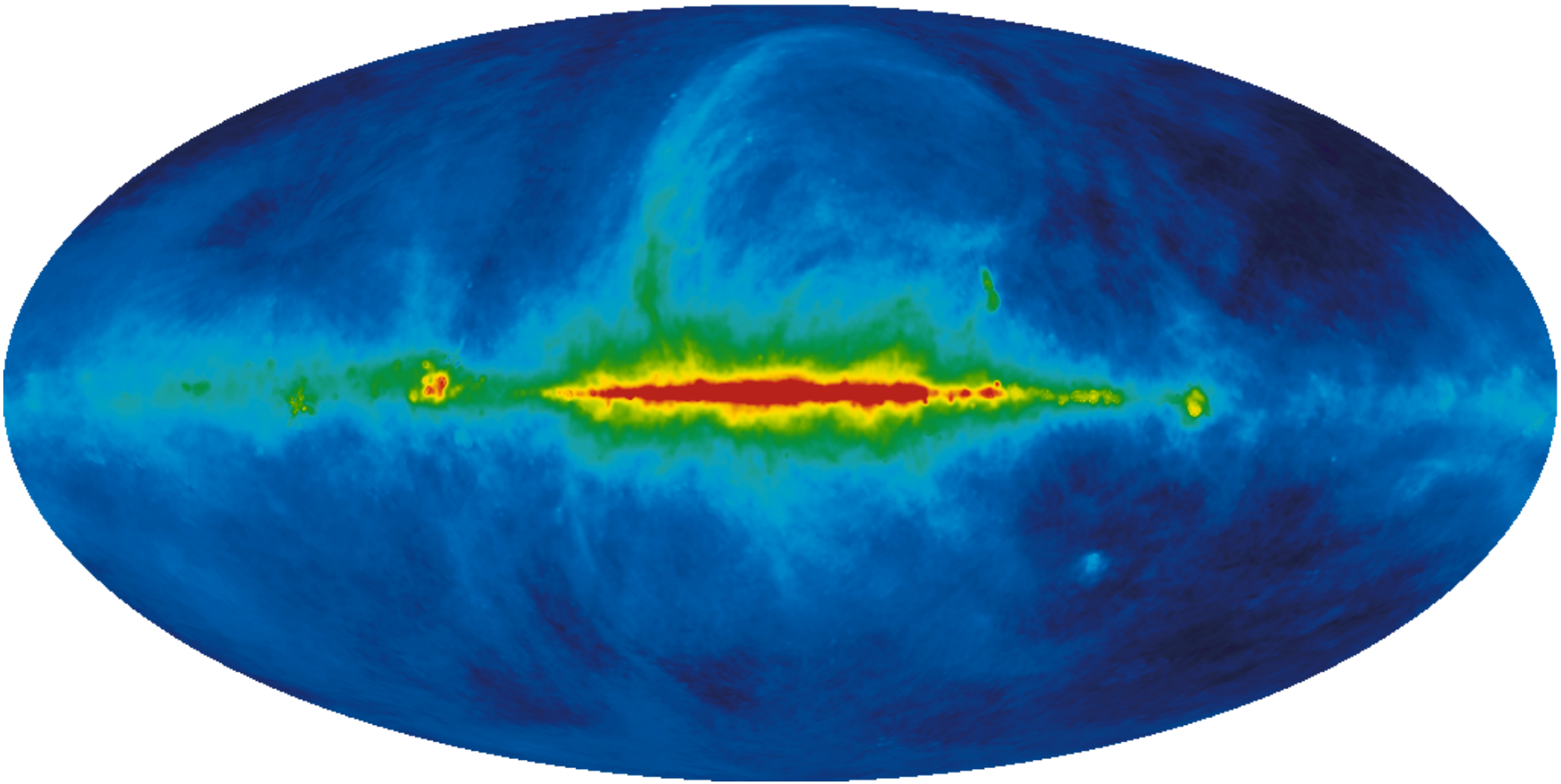

Full-sky survey at 408 MHz, dominated by synchrotron emission.
Concentrated to inner plane, features prominent loop structures.

lambda.gsfc.nasa.gov

"Free–Free" Emission (H–α proxy)

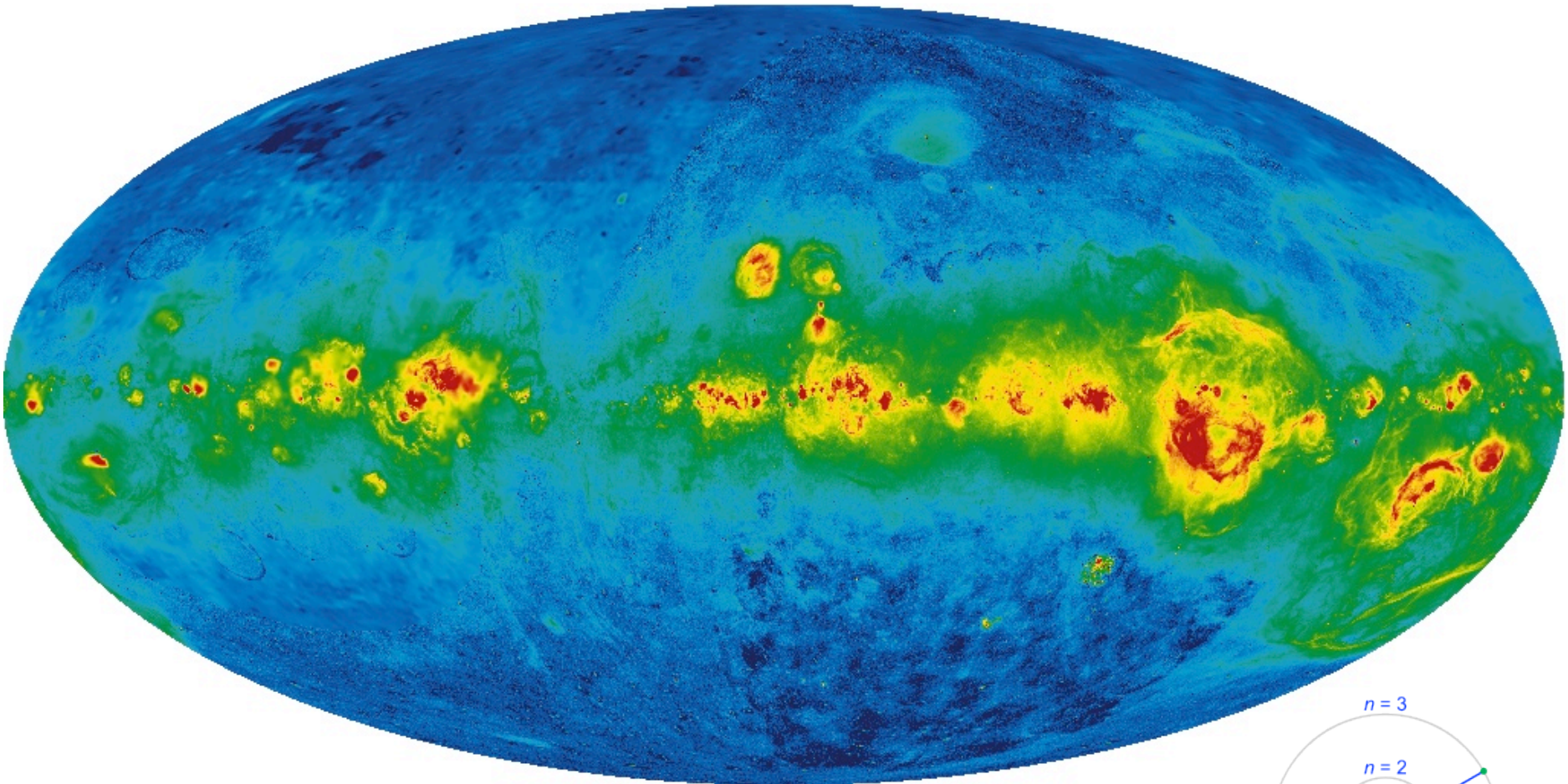

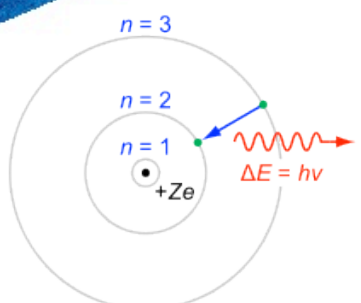

Full sky compilation of H-α emission, tracing light emitted by the warm ionized medium in the Milky Way. $\lambda = 656$ nm. Only traces nearby gas due to extinction.

lambda.gsfc.nasa.gov

Thermal Dust Emission (Model)

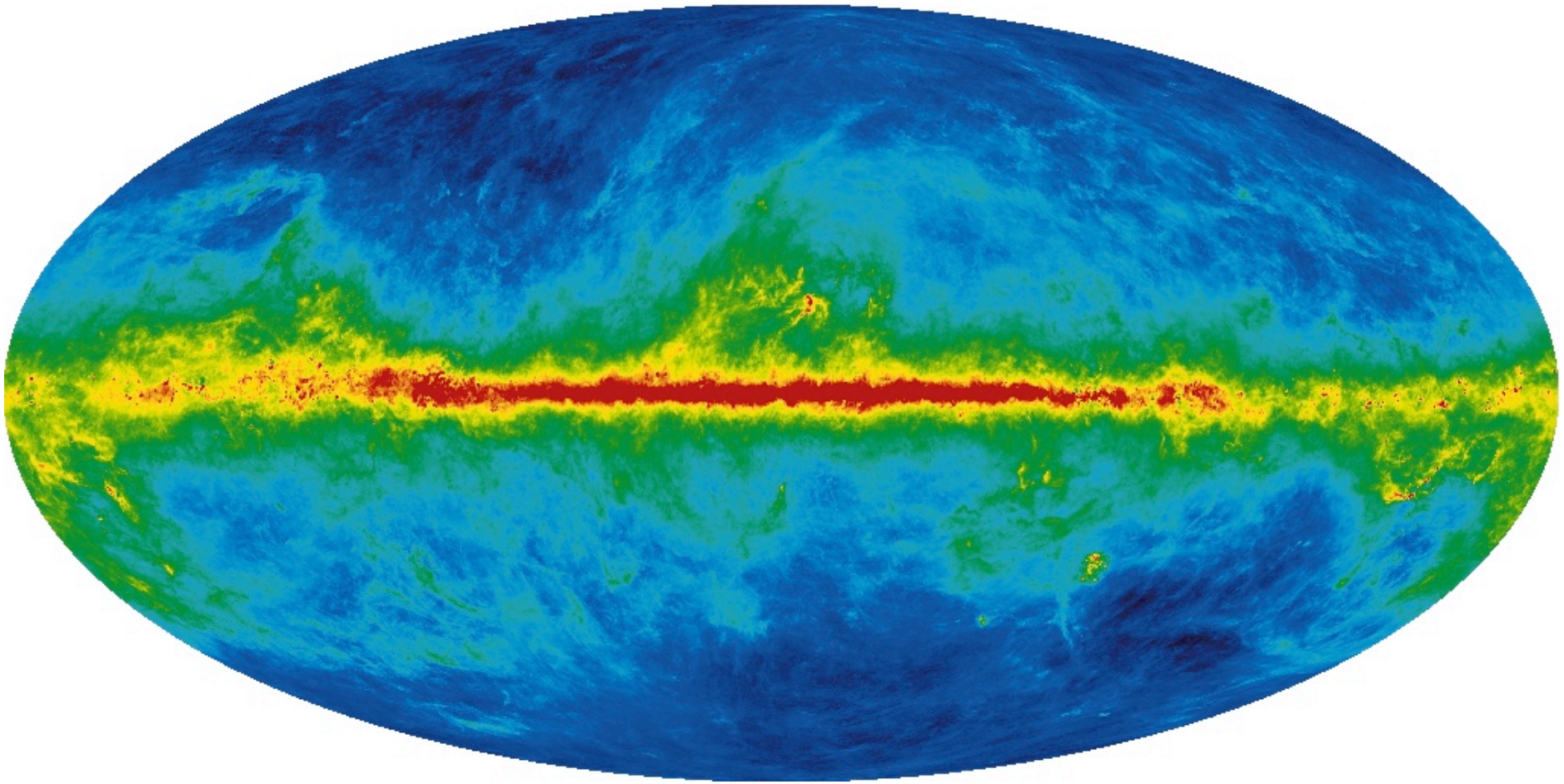

Full sky map of FIR emission compiled by Finkbeiner et al. from a combination of IRAS, COBE-DIRBE, and COBE-FIRAS data.

lambda.gsfc.nasa.gov

WMAP Full-Sky Maps: 5 Bands

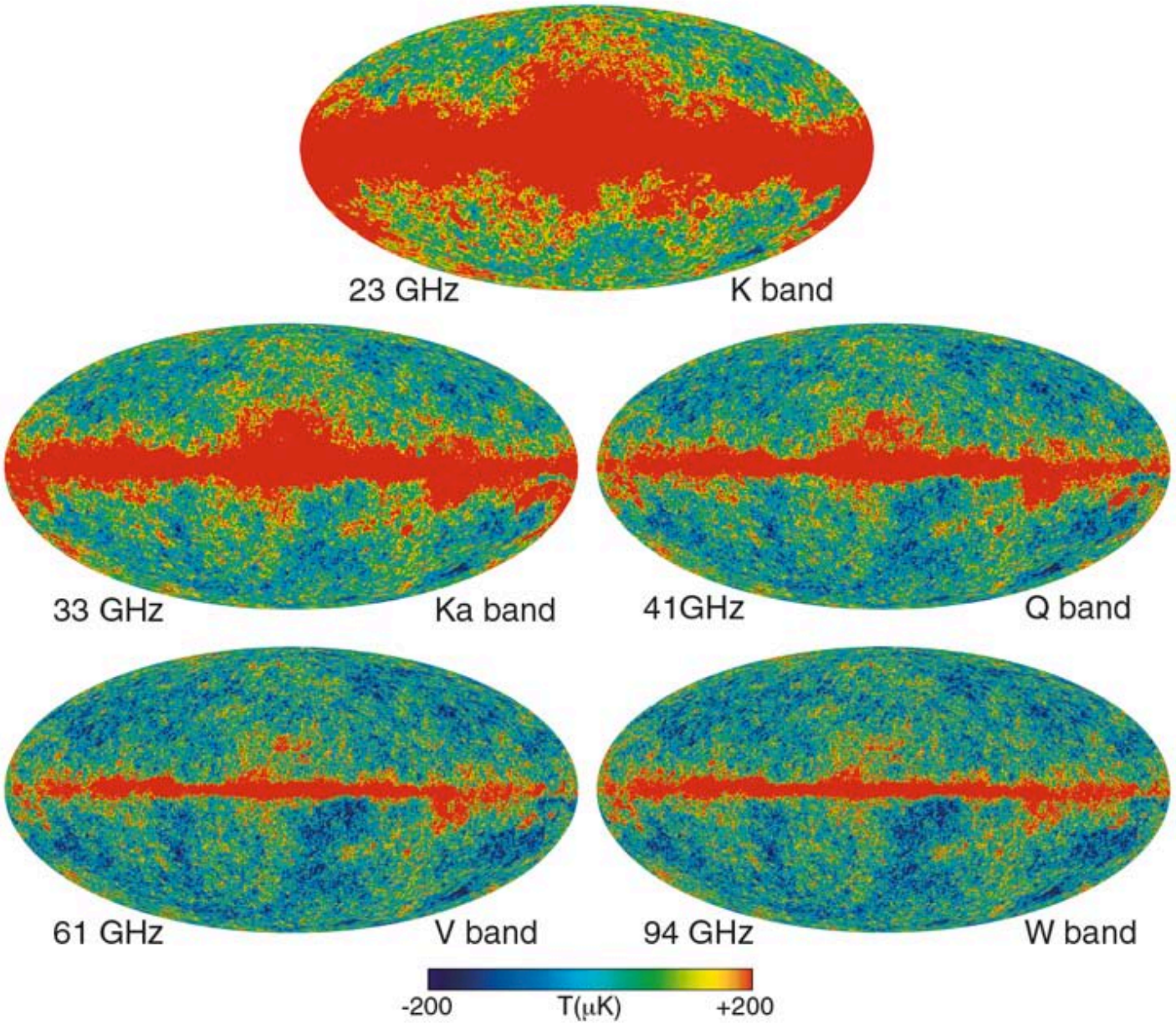

Planck Full-Sky Maps: 9 Bands

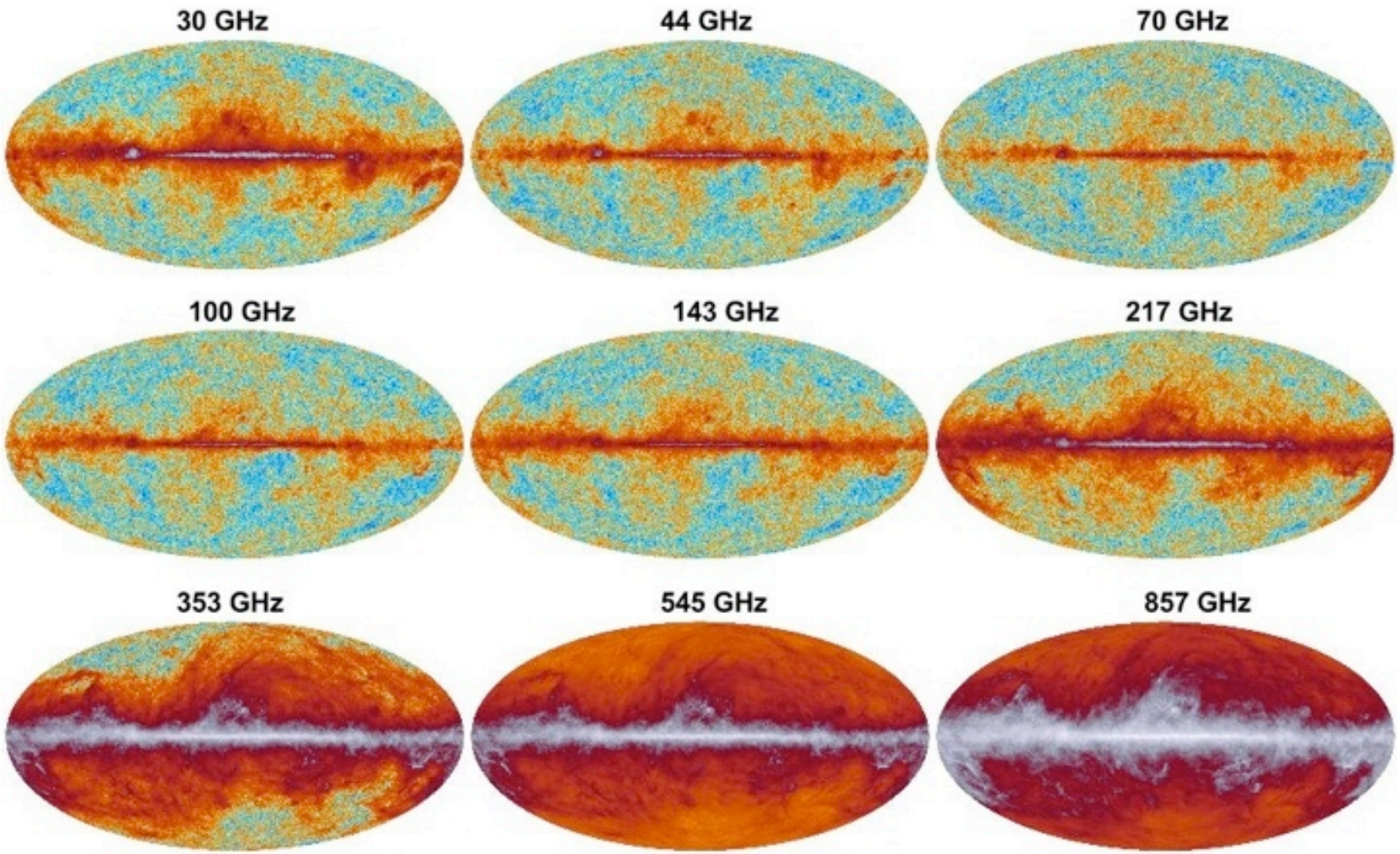

WMAP 23 GHz Temperature

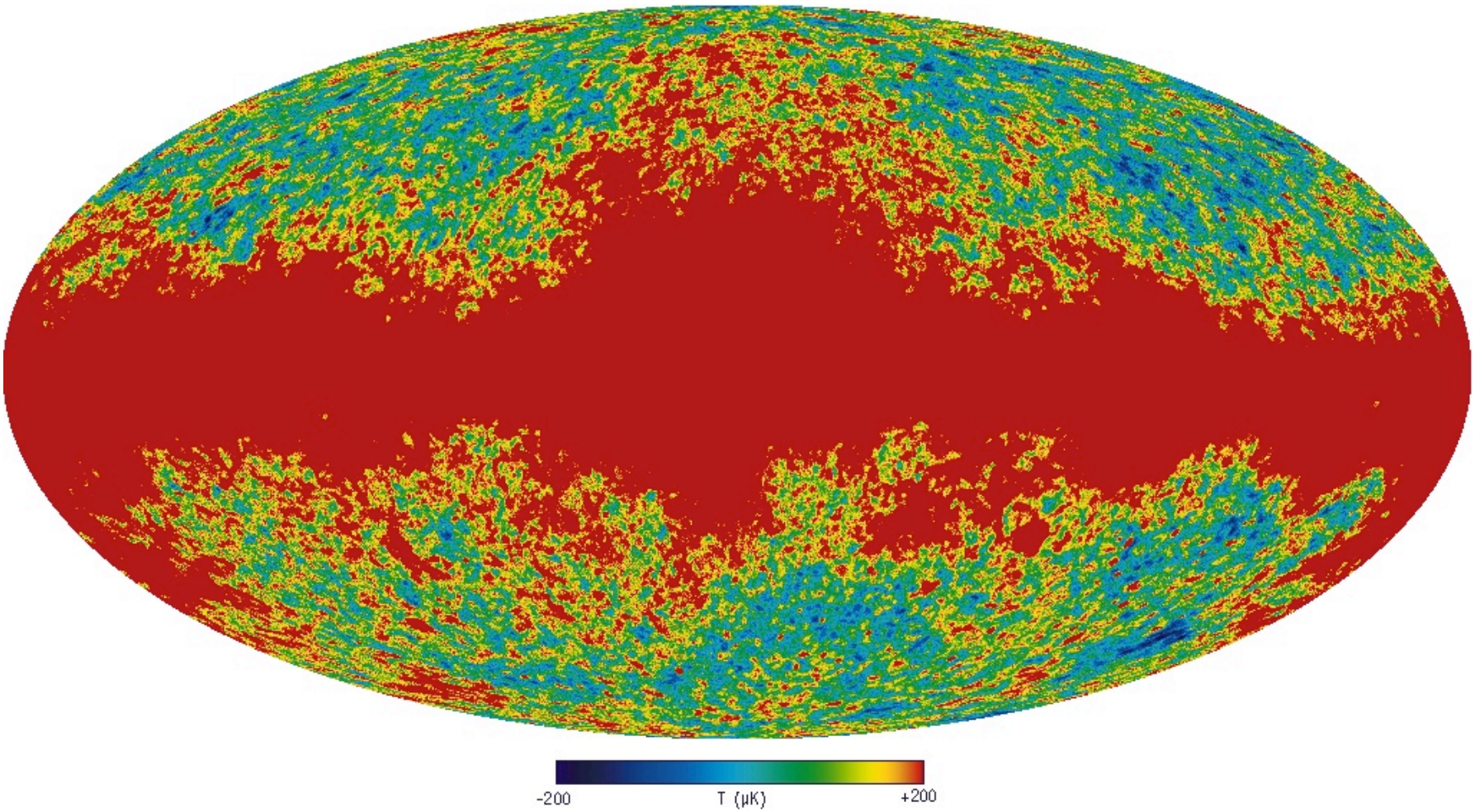

WMAP 33 GHz Temperature

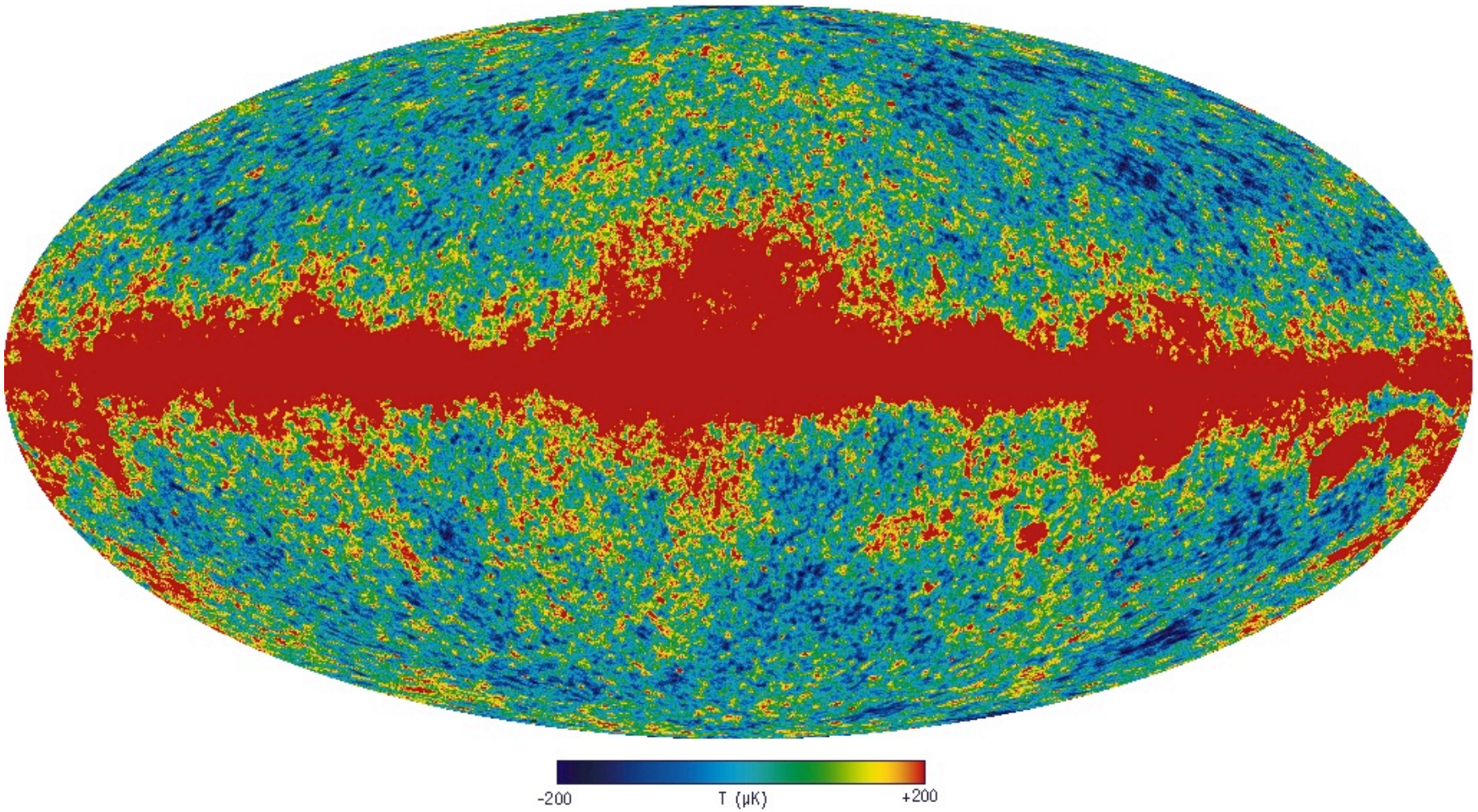

WMAP 41 GHz Temperature

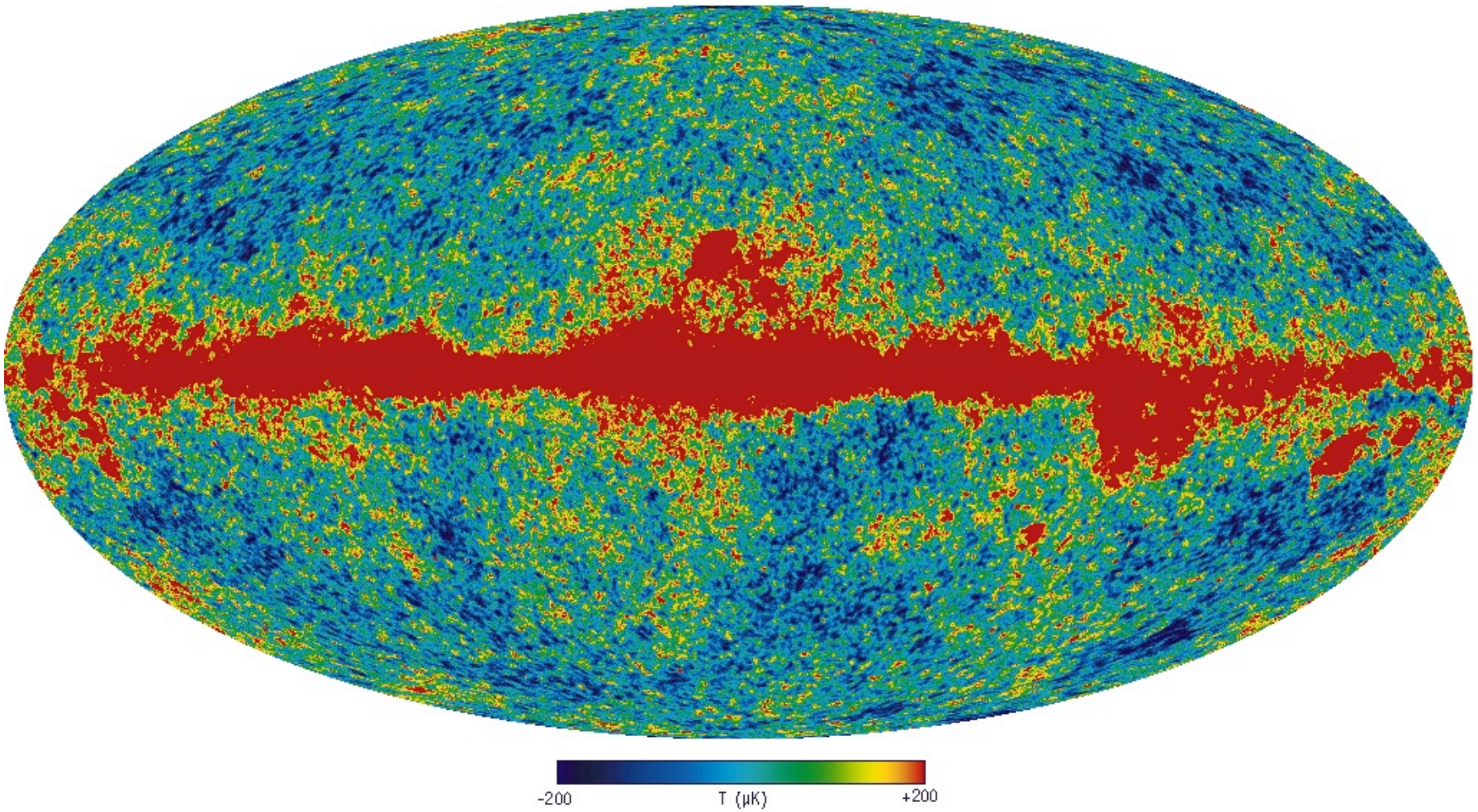

WMAP 61 GHz Temperature

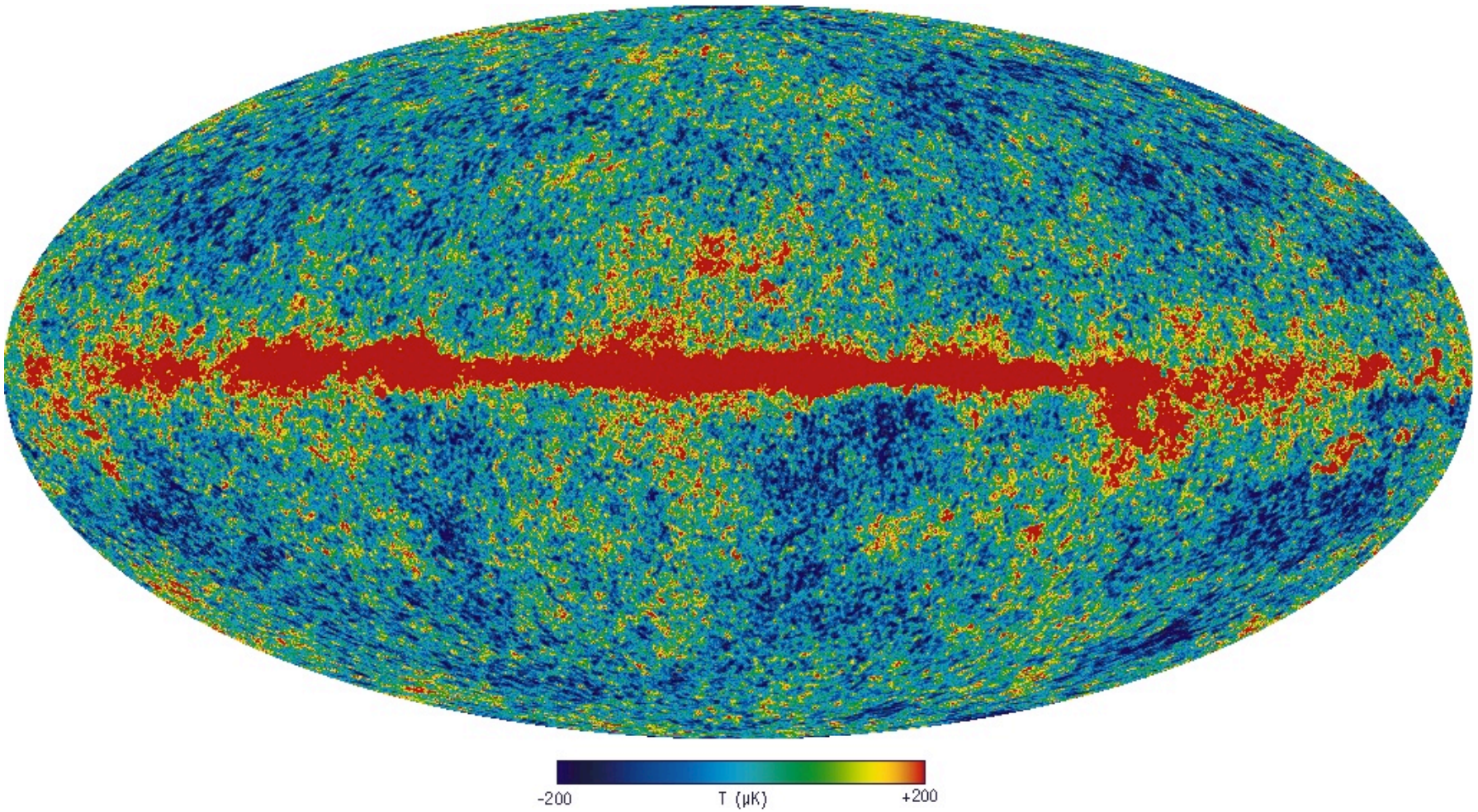

WMAP 94 GHz Temperature

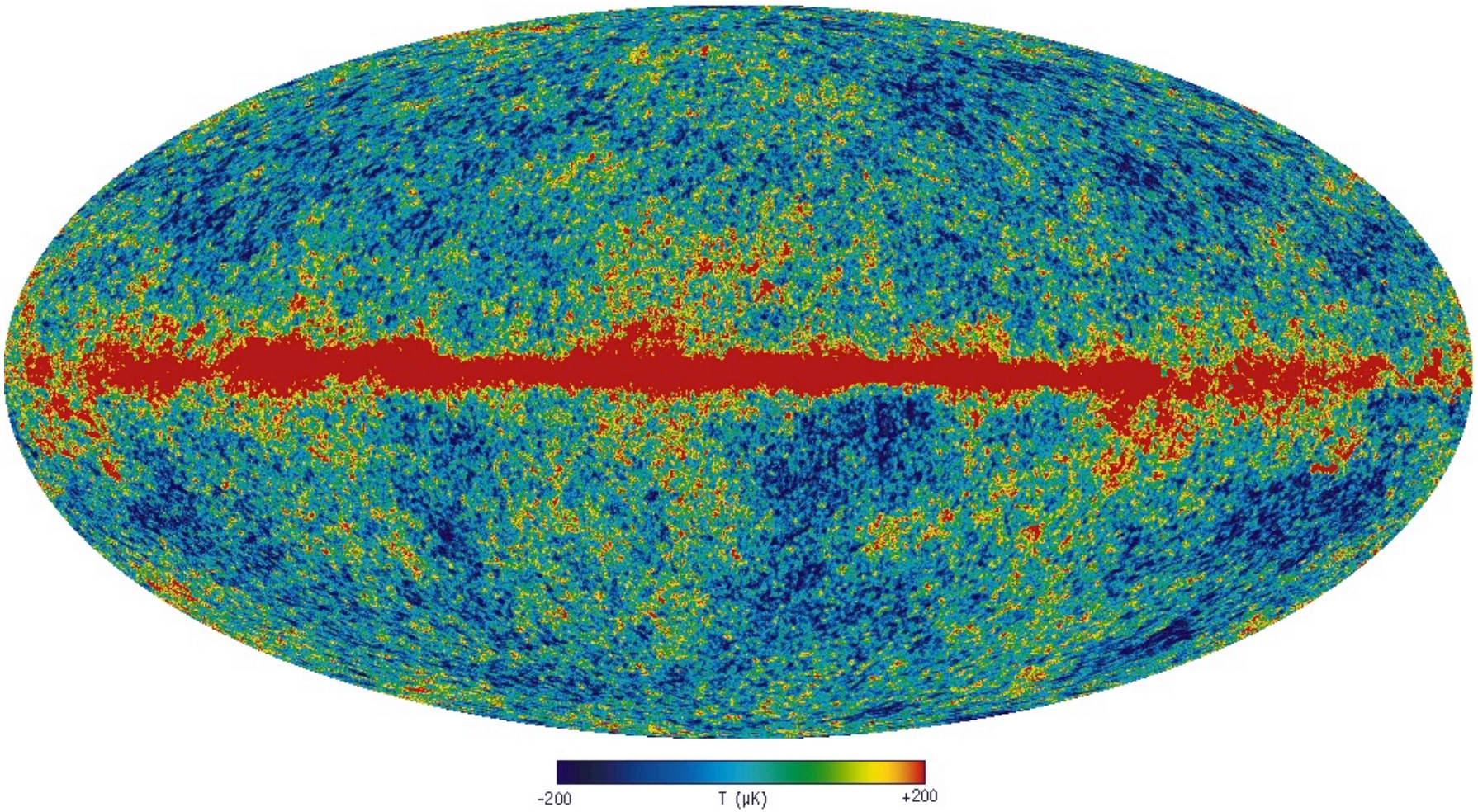

5 Frequency Linear Combination ("ILC")

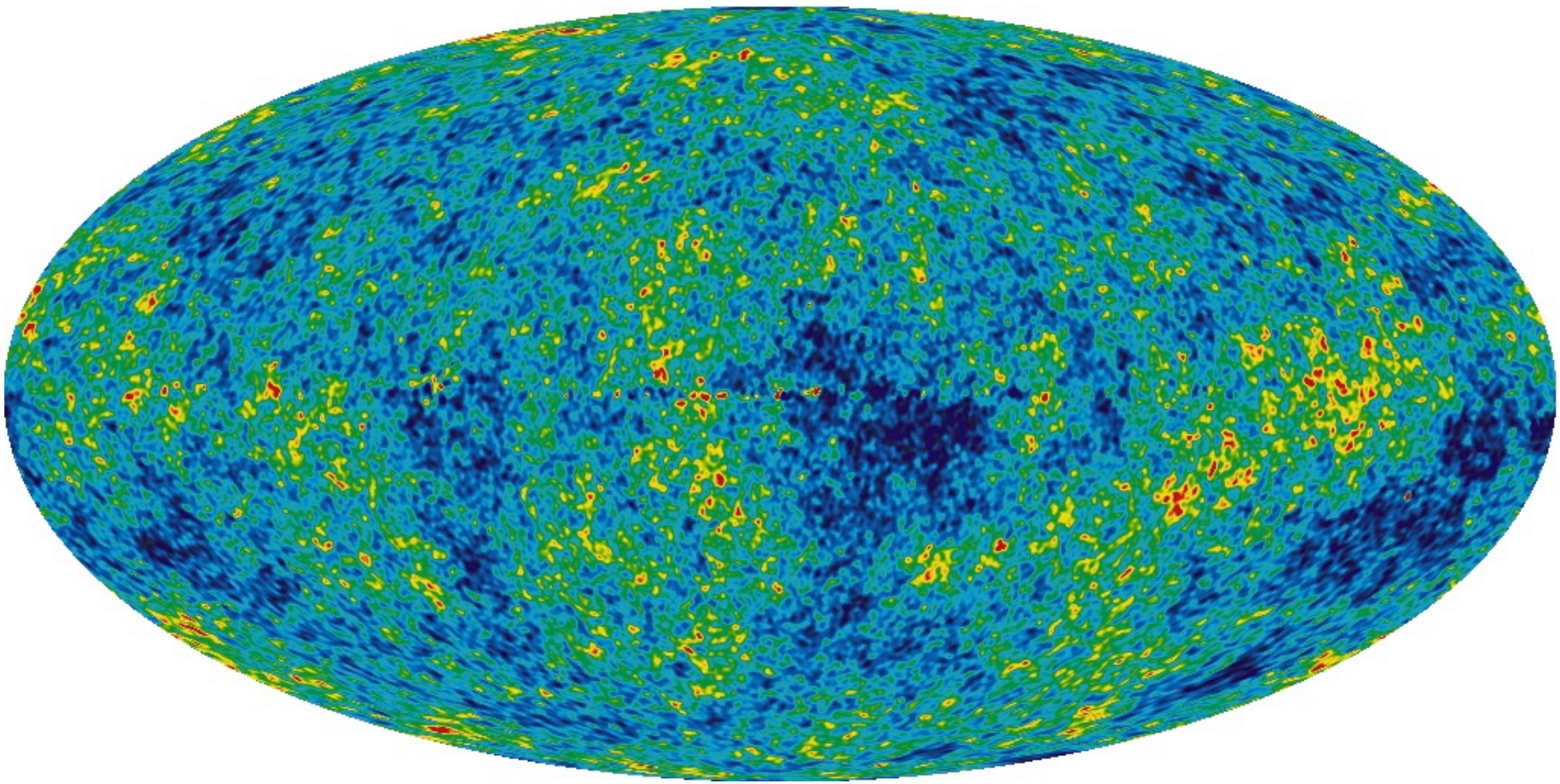

Linear combination of 5 WMAP bands that minimizes map variance subject to the constraint that [CMB]=1. *Fine print: sky divided into 12 regions by hand; subject to foreground-CMB covariance bias.*

WMAP "$B_i - B_j$" Color Map

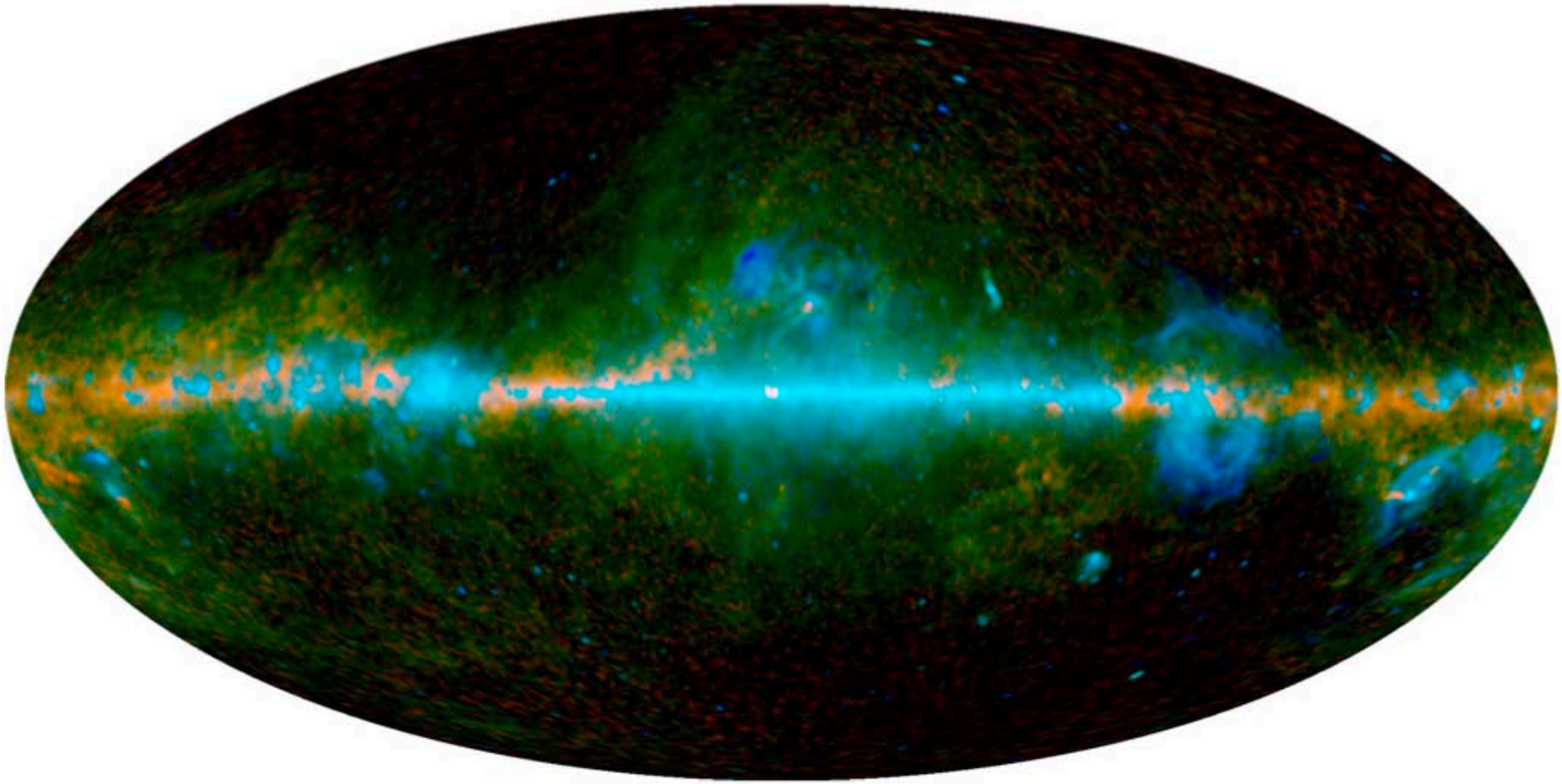

Orange - regions where dust is dominant (W−V color).
Blue - regions where free-free is dominant (Q−W color).
Green - regions where synchrotron is dominant (K−Q color).

Model Synchrotron at 23 GHz

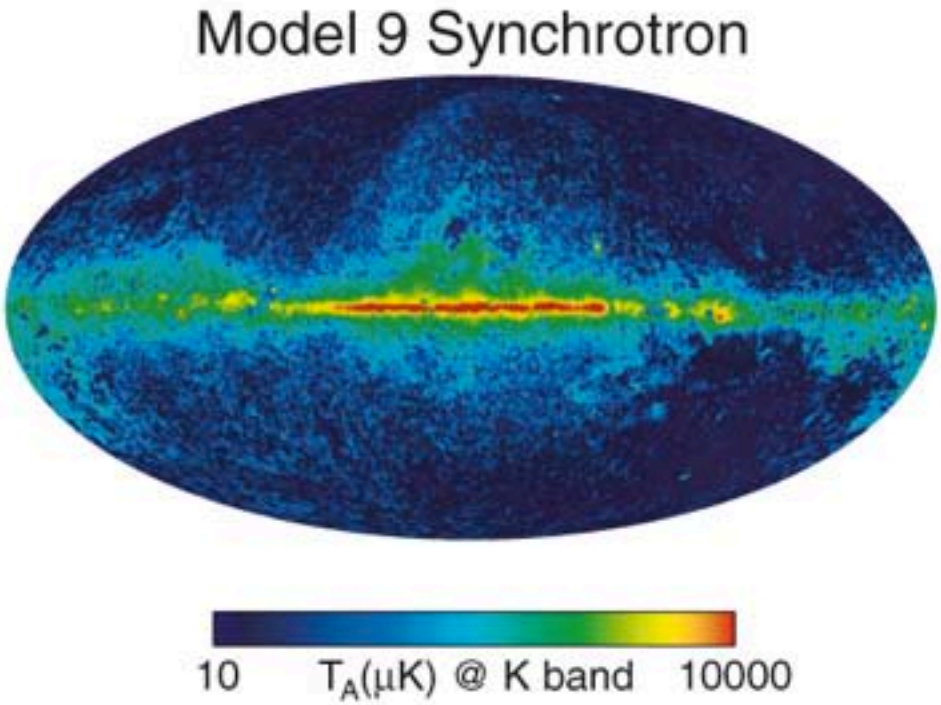

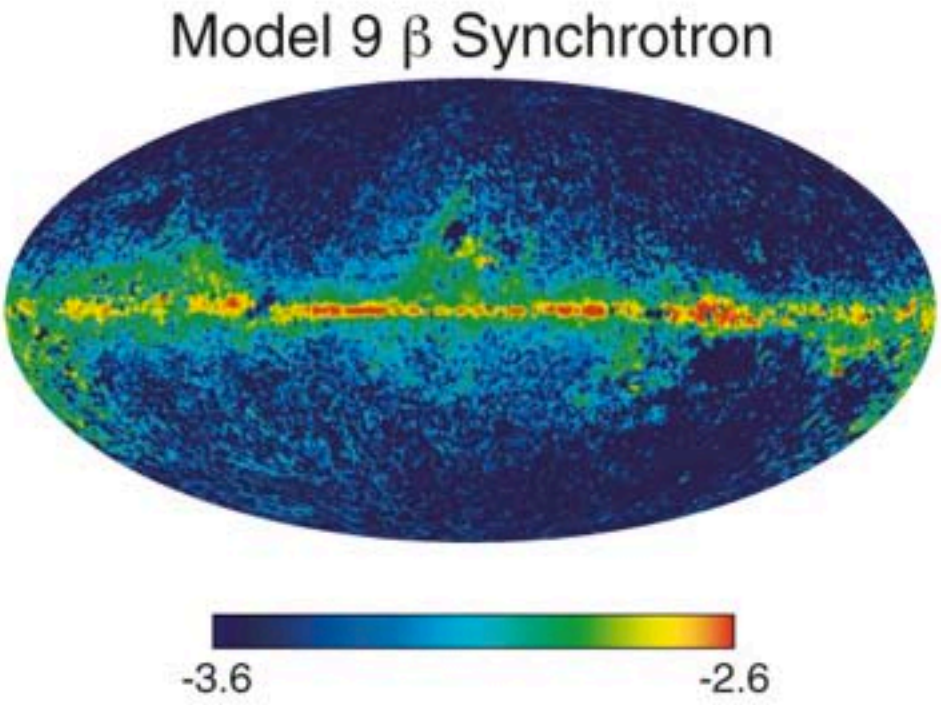

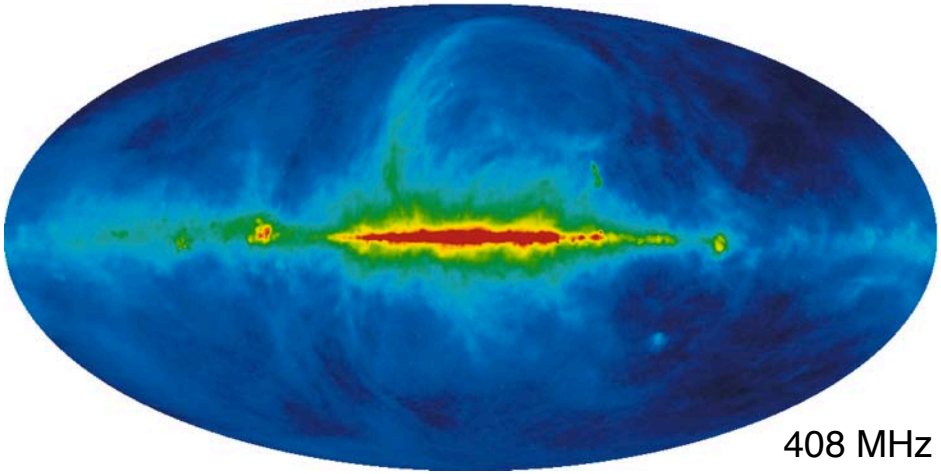

Microwave synchrotron based on combined spectral & spatial modeling.

Bennett et al. arXiv:1212.5225.

Model Free-Free at 23 GHz

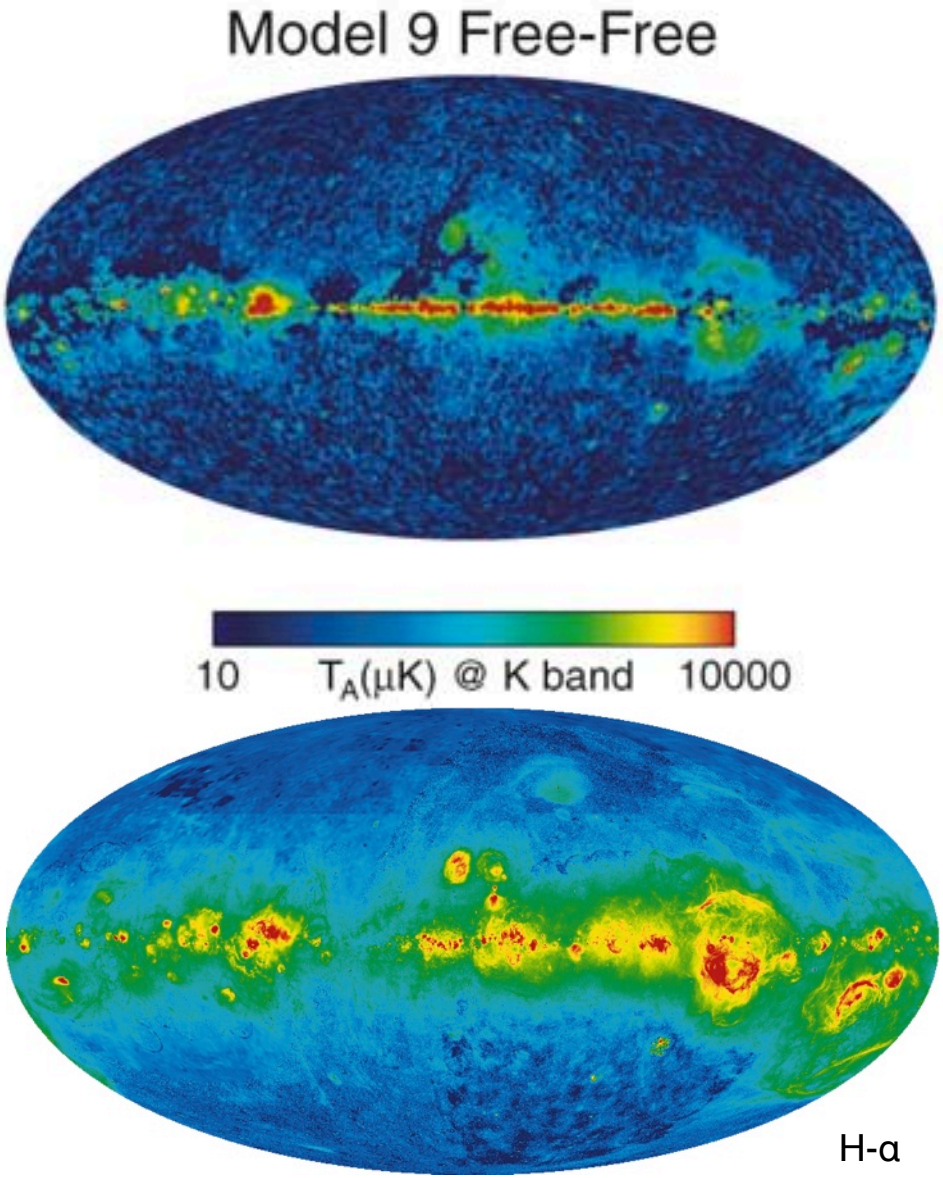

Microwave free-free based on combined spectral & spatial modeling.

Bennett et al. arXiv:1212.5225.

Free-free (radio) emission does not suffer from extinction.

Model Dust at 94 GHz

Model 9 Thermal Dust

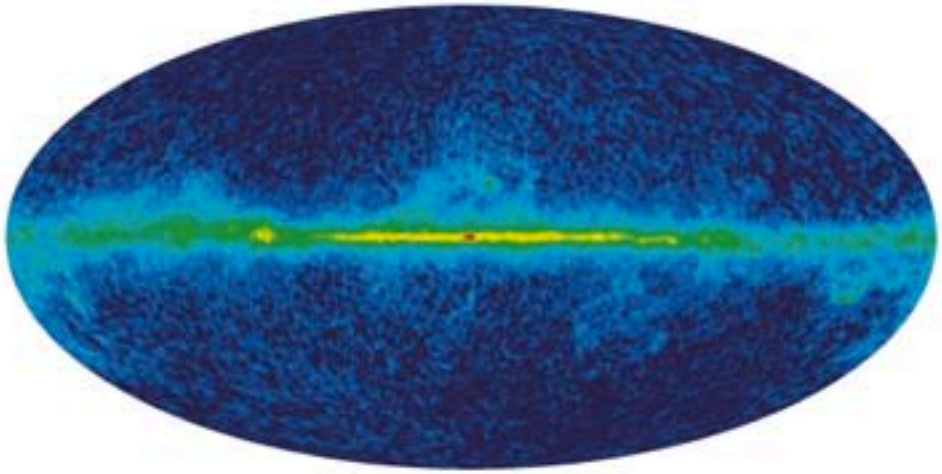

Mean Model T_{dust} – FDS model 8

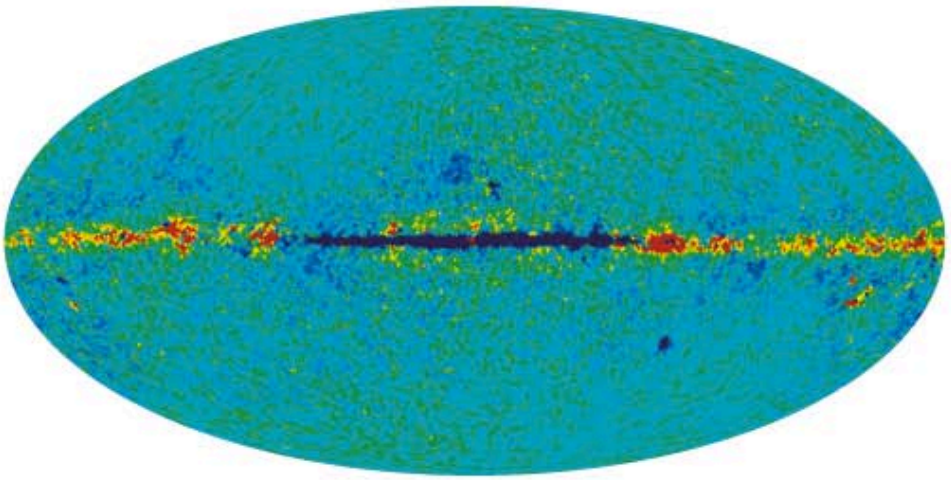

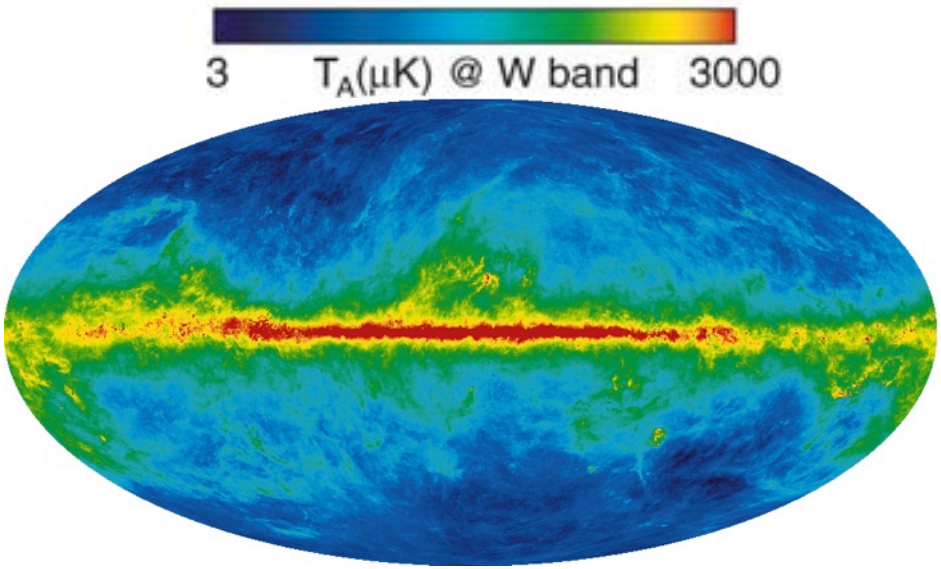

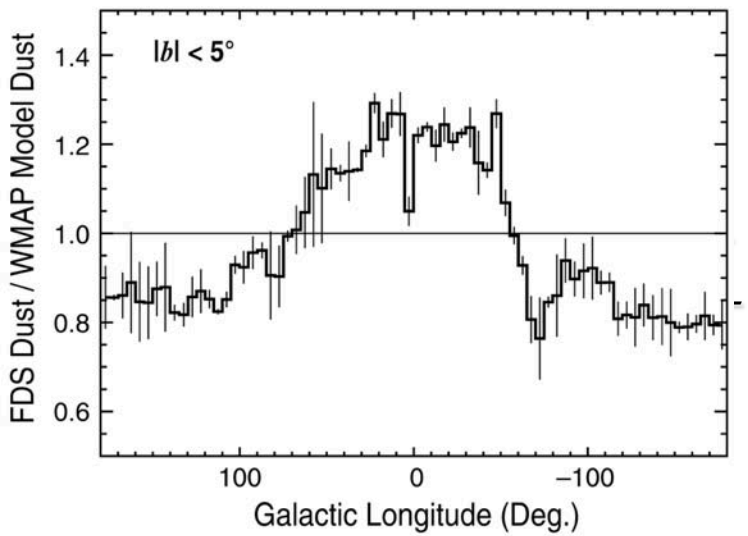

Unpolarized Foreground Summary

Removing foreground emission for cosmology studies is relatively simple because CMB anisotropy dominates structure in ~40-150 GHz range.

What luck!

Separating foreground components in the microwave regime is *very* difficult. Generalization of the thermal/non-thermal separation problem at lower frequencies.

Current efforts certainly have systematic errors, but are still informative.

Galactic Foregrounds – Polarized

WMAP Full-Sky Polarization: 5 Bands

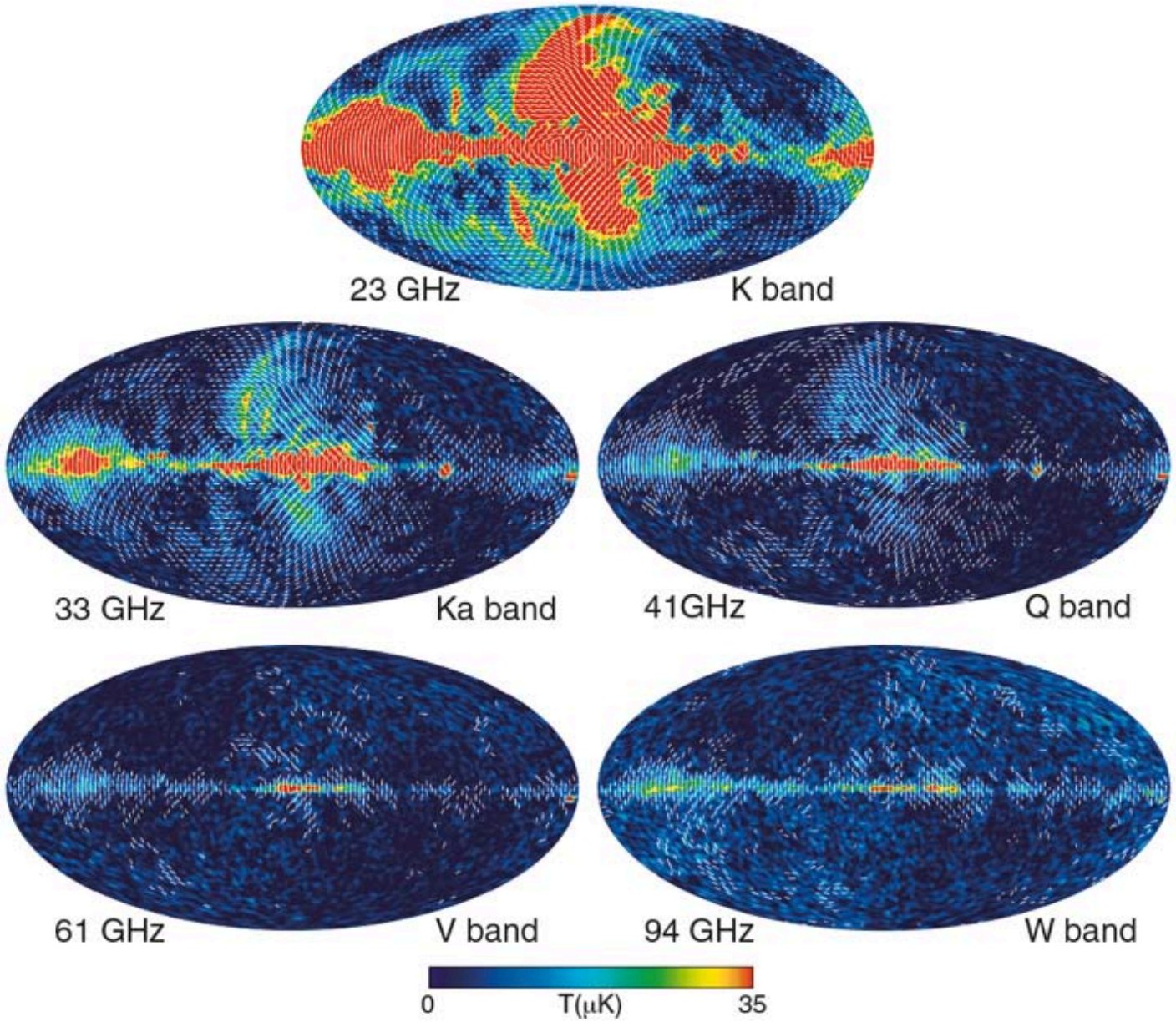

Radio Depolarization

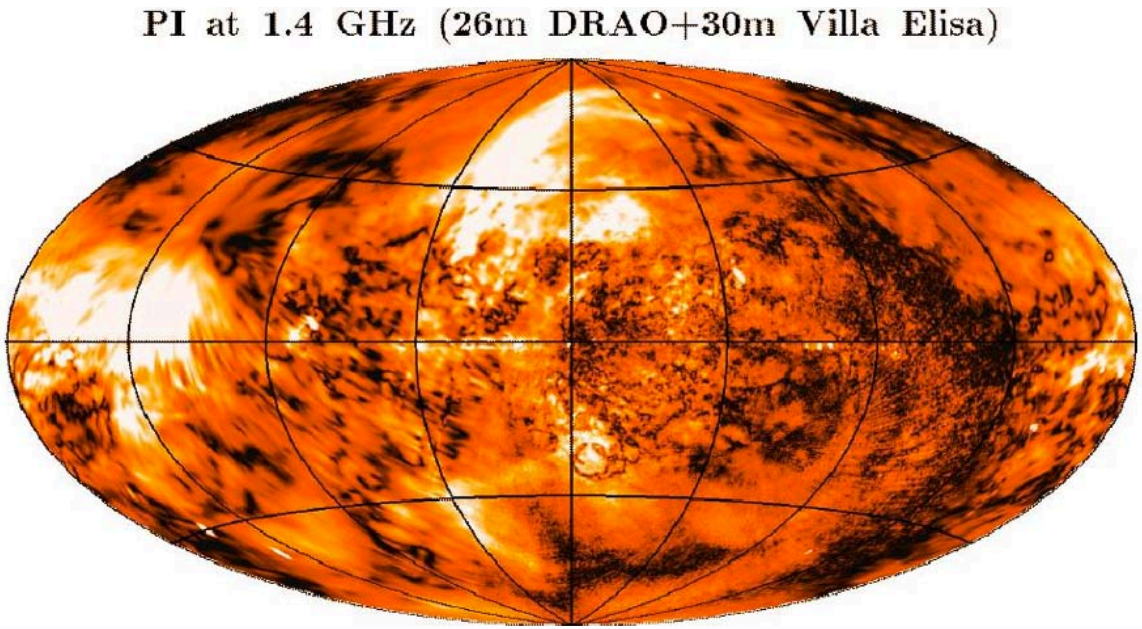

Radio (1.4 GHz) emission is strongly depolarized in the inner galaxy due to Faraday rotation.

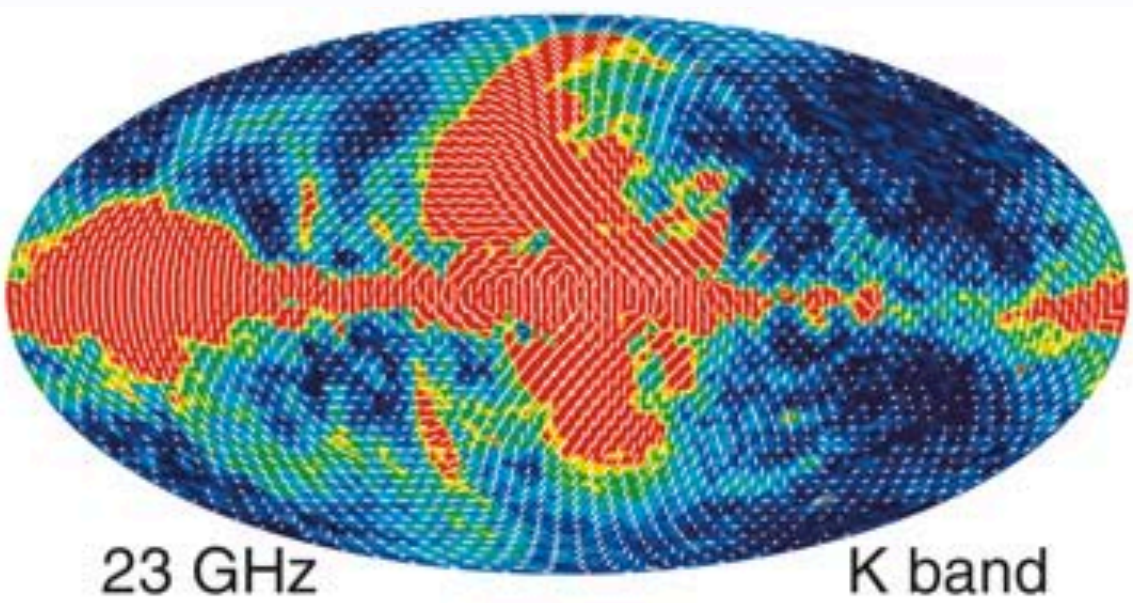

Microwave emission suffers negligible Faraday rotation.

WMAP Polarization Spectra

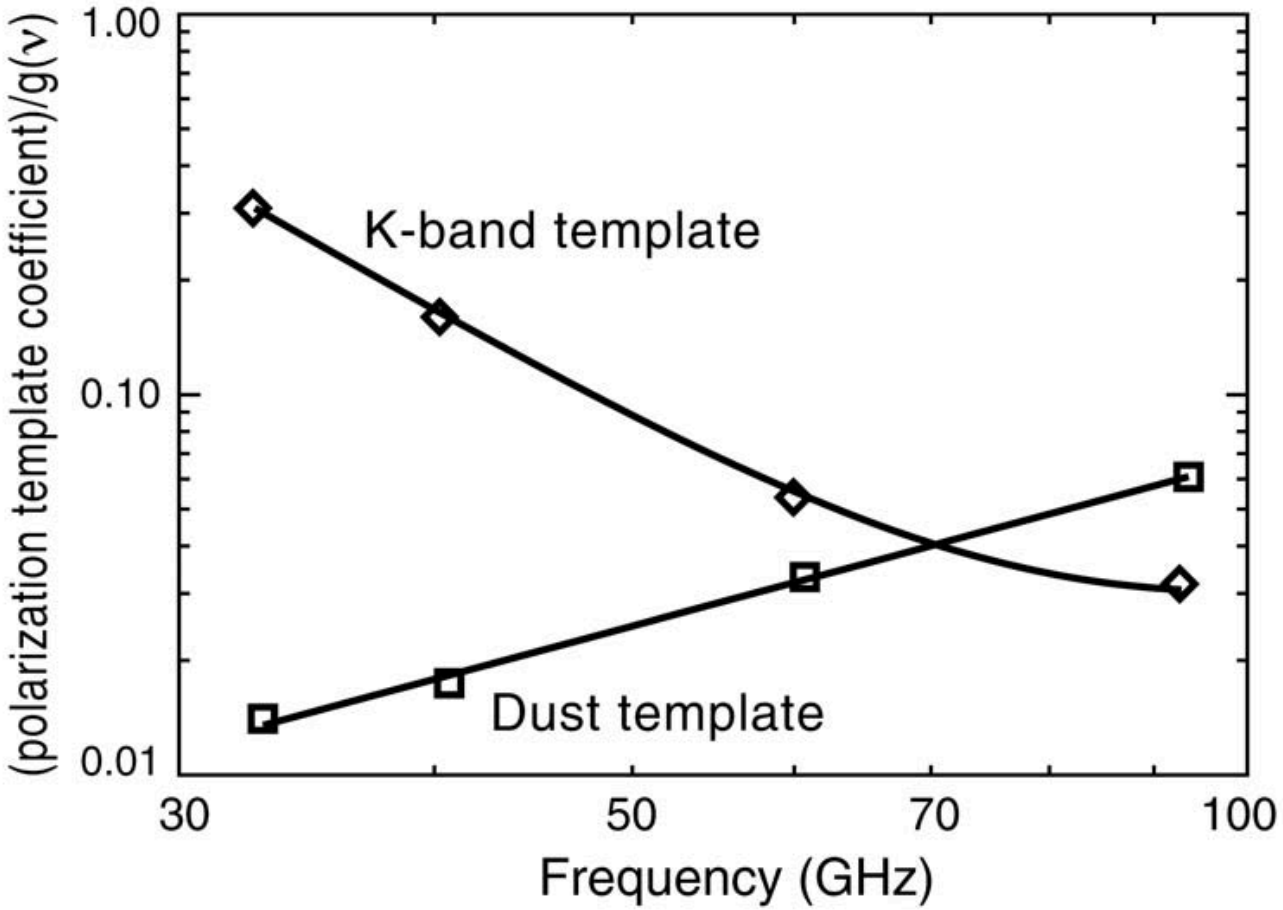

Fit 23 GHz map as a template to higher frequency WMAP bands. Odd feature: spectrum flattens as frequency increases - counter to naive expectations! Interpreted as a dust component spatially correlated with polarized synchrotron and not by the model dust template.

Inflation and Gravity Waves – I

- Inflation predicts two forms of fluctuations:
  - Scalar modes (density perturbations) with slope n_s:
    - generate CMB anisotropy and lead to structure formation
  - Tensor modes (gravity waves) with slope n_t:
    - generate CMB anisotropy but do not contribute to structure formation
- Gravity wave amplitude, r, proportional to energy scale of inflation:

$$r^{1/4} \propto \frac{V_\phi^{1/4}}{m_{pl}} = \frac{E_{\text{infl}}}{3.3\times10^{16}\,\text{GeV}} \text{ with } r \equiv \frac{P(k_0)_{tensor}}{P(k_0)_{scalar}}$$

- Both types of fluctuations contribute to CMB temperature anisotropy:

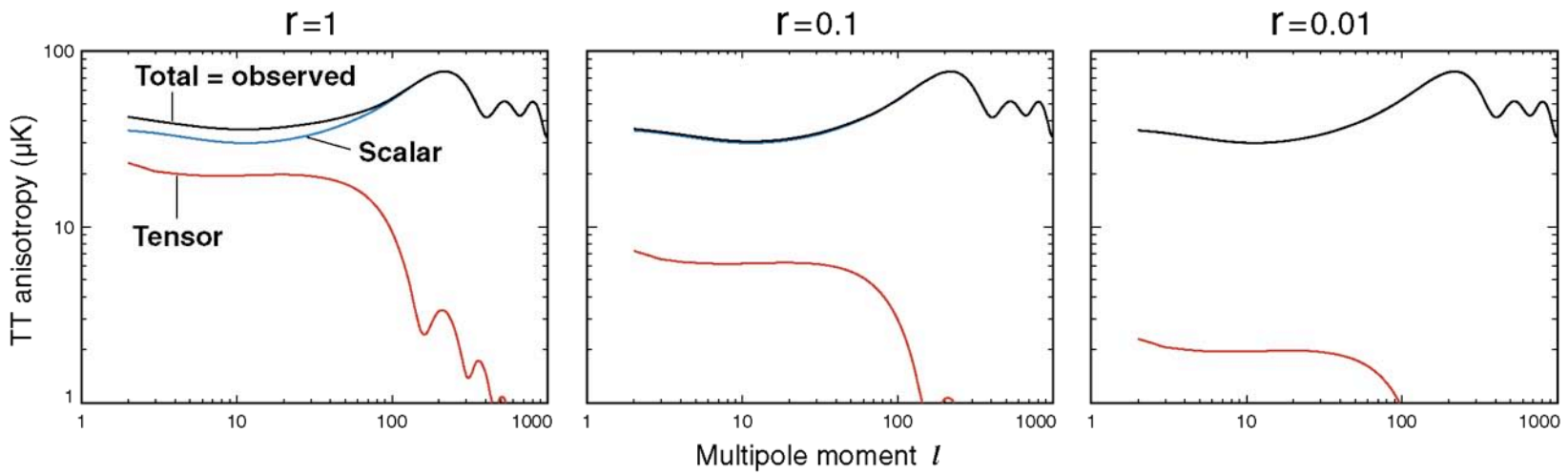

Inflation and Gravity Waves – II

- Both types of fluctuations contribute to CMB polarization anisotropy:
  - Scalar modes produce only "E-mode" polarization patterns, by symmetry
  - Tensor modes produce both "E-mode" and "B-mode" polarization patterns (see below)
- The observation of B-mode polarization uniquely separates scalar and tensor modes from inflation and measures the energy scale of inflation.
- *Only* known probe of physics at E ~ 10^{16} GeV… *12 orders of magnitude higher than planned accelerators.*

E – scalar+tensor

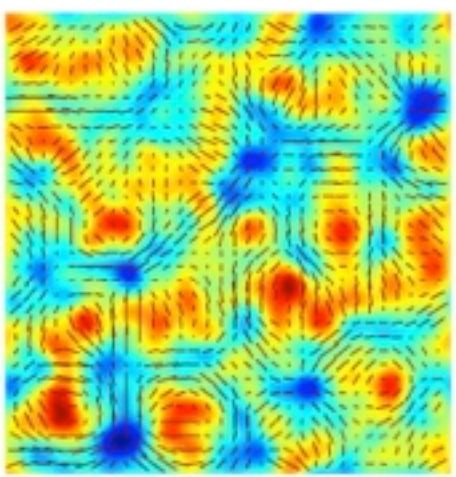

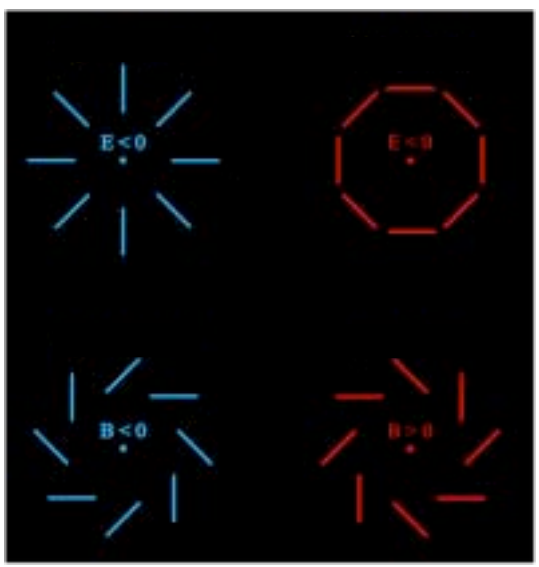

B – tensor only

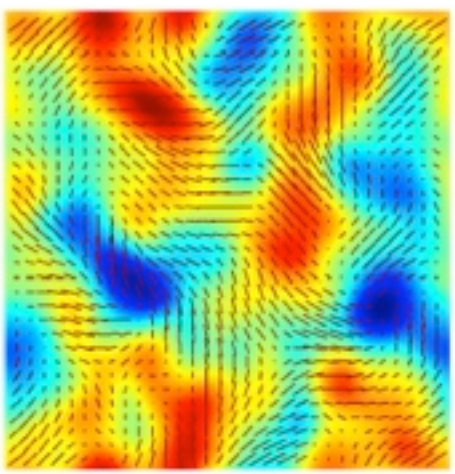

Predicted Polarization Spectra, r=1.0

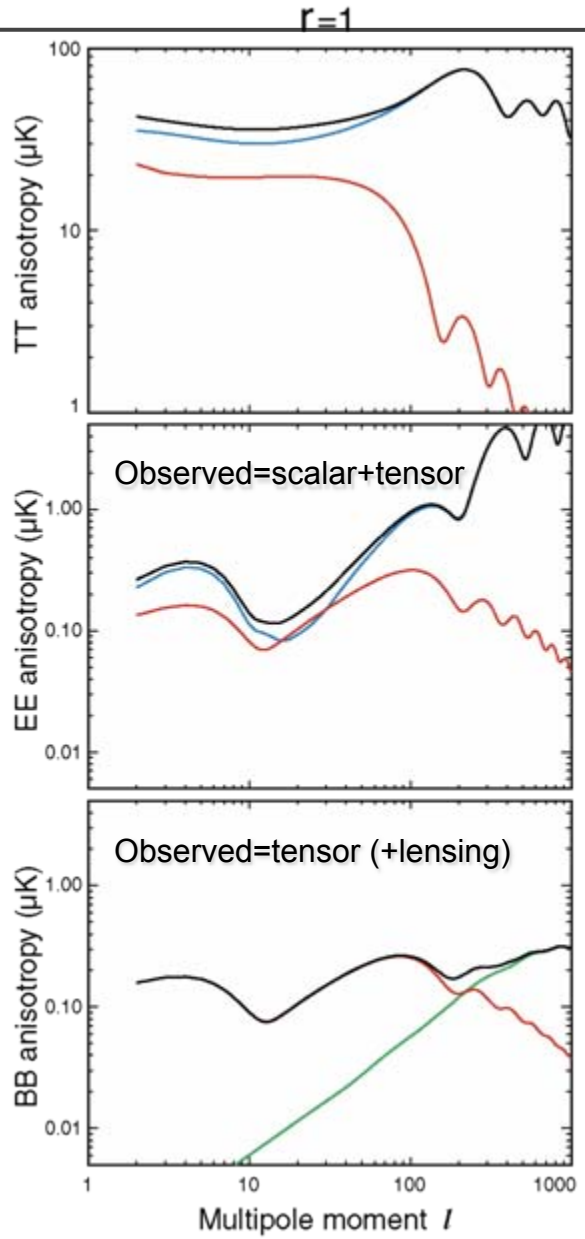

Temperature spectrum
(as before)

E-mode polarization spectrum,
scalar (blue) & tensor (red) terms

B-mode polarization spectrum,
tensor (red) & gravitational lensing (green)
terms

Predicted Polarization Spectra, r=0.1

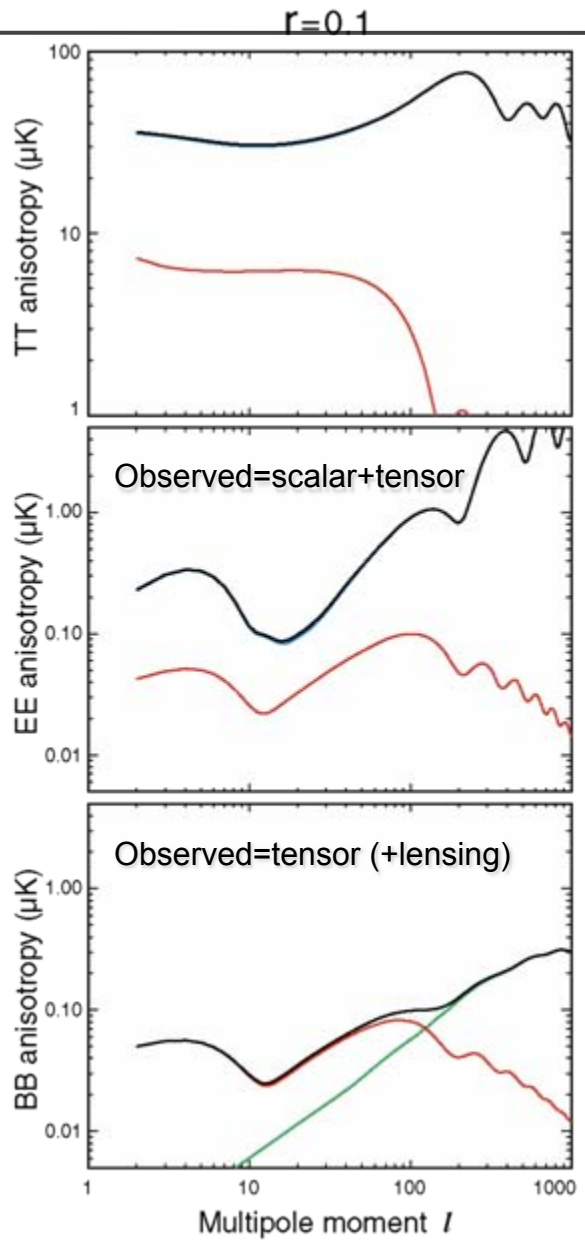

Temperature spectrum
(as before)

E-mode polarization spectrum,
scalar (blue) & tensor (red) terms

B-mode polarization spectrum,
tensor (red) & gravitational lensing (green)
terms

Predicted Polarization Spectra, r=0.01

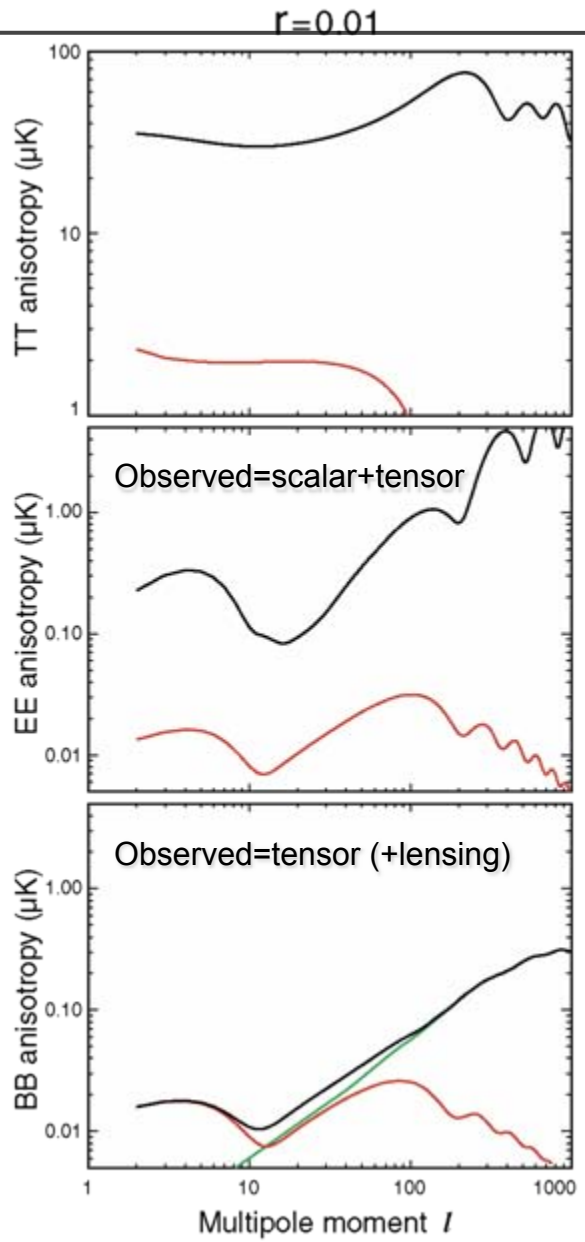

Temperature spectrum
(as before)

E-mode polarization spectrum,
scalar (blue) & tensor (red) terms

B-mode polarization spectrum,
tensor (red) & gravitational lensing (green)
terms

BICEP2 – Polarization @ 150 GHz

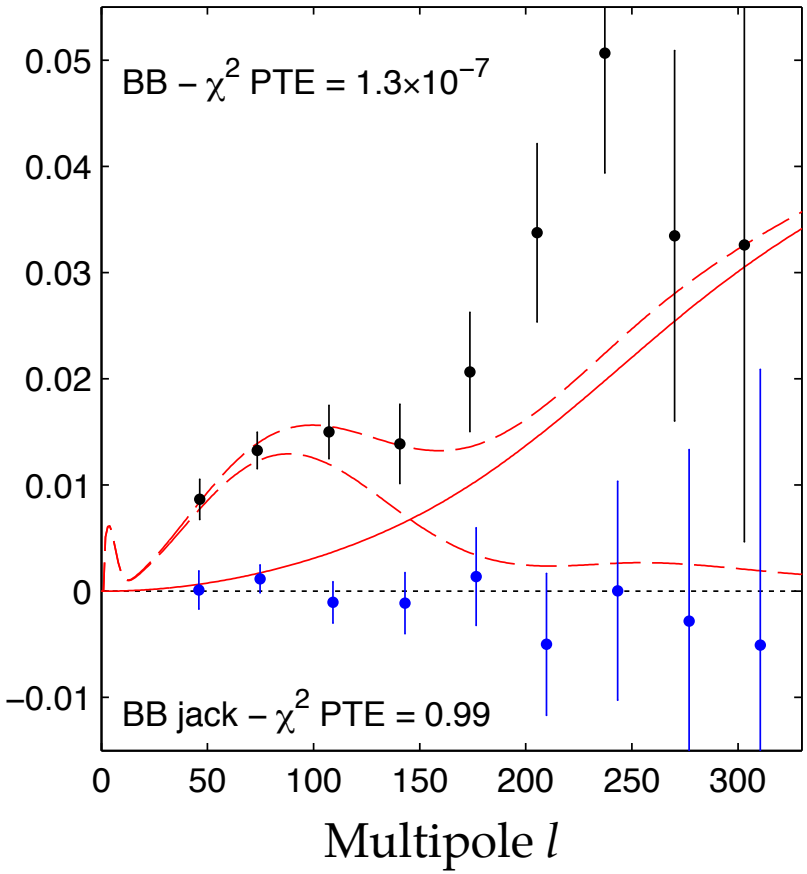

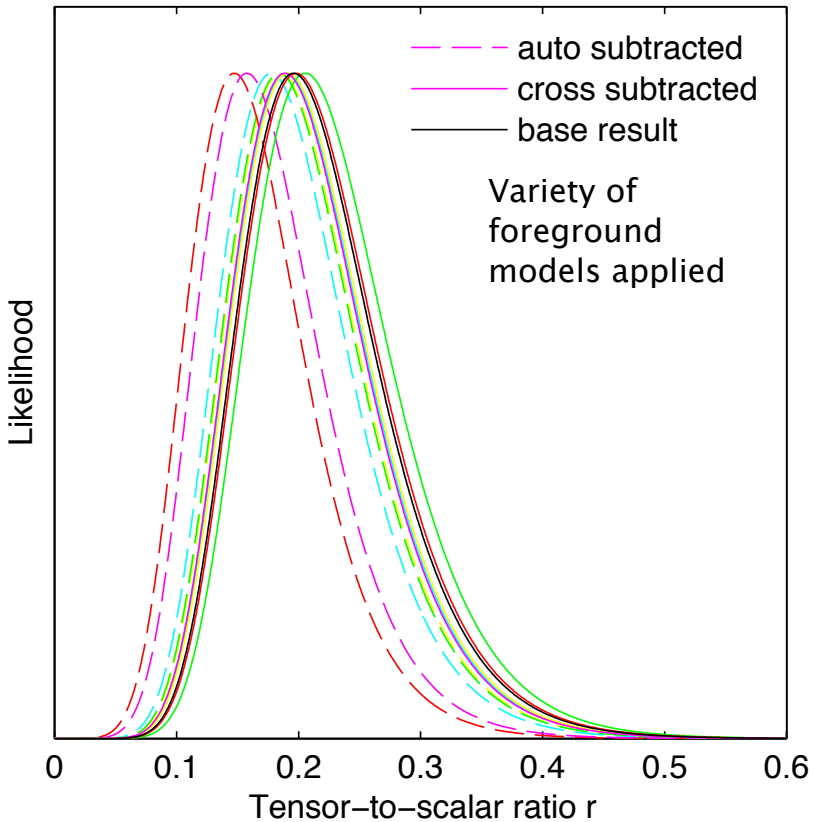

The BICEP2 team reports detection of B-mode polarization (right) and argues that it *cannot* be explained by foreground emission from synchrotron or dust (right).

Big surprise: $r \approx 0.2$, higher than the limit reported by WMAP & Planck: ($r < 0.12$).

Planck & BICEP2 – I

Planck intermediate results. XXX. The angular power spectrum of polarized dust emission at intermediate and high Galactic latitudes

2014 Sep 22 (today!)

Galactic latitudes with low dust column densities. We show that even in the faintest dust-emitting regions there are no "clean" windows in the sky where primordial CMB *B*-mode polarization measurements could be made without subtraction of foreground emission. Finally, we investigate the level of dust polarization in the specific field recently targeted by the BICEP2 experiment. Extrapolation of the *Planck* 353 GHz data to 150 GHz gives a dust power $\mathcal{D}_\ell^{BB} \equiv \ell(\ell+1)C_\ell^{BB}/(2\pi)$ of $1.32 \times 10^{-2}\,\mu\mathrm{K}^2_{\mathrm{CMB}}$ over the multipole range of the primordial recombination bump ($40 < \ell < 120$); the statistical uncertainty is $\pm 0.29 \times 10^{-2}\,\mu\mathrm{K}^2_{\mathrm{CMB}}$ and there is an additional uncertainty $(+0.28, -0.24) \times 10^{-2}\,\mu\mathrm{K}^2_{\mathrm{CMB}}$ from the extrapolation. This level is the same magnitude as reported by BICEP2 over this ℓ range, which highlights the need for assessment of the polarized dust signal even in the cleanest windows of the sky. The present uncertainties are large and will be reduced through an ongoing, joint analysis of the *Planck* and BICEP2 data sets.

"...We show that even in the faintest dust-emitting regions there are no "clean" windows in the sky where primordial CMB B-mode polarization measurements could be made without subtraction of foreground emission."

"...This level is the same magnitude as reported by BICEP2 over this l range, which highlights the need for assessment of the polarized dust signal even in the cleanest windows of the sky. "

Planck & BICEP2 – II

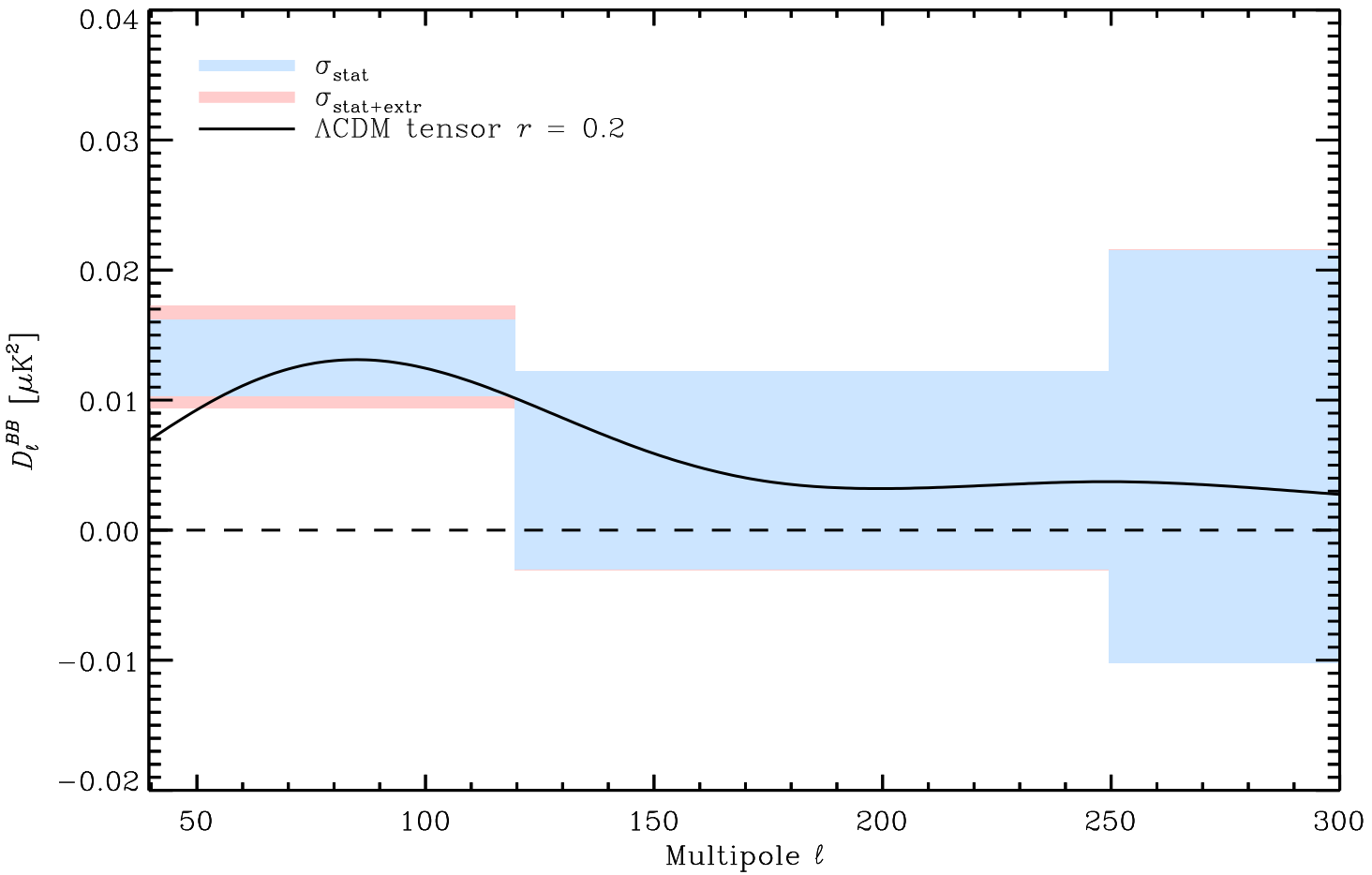

Blue boxes - 353 GHz BB dust spectrum extrapolated to 150 GHz (BICEP2 band) with 1σ uncertainties (pink includes systematic errors). Black curve is an r=0.2 ΛCDM model spectrum....

Extragalactic Foregrounds – SZ

Probing Gas with Planck SZ Map(s)

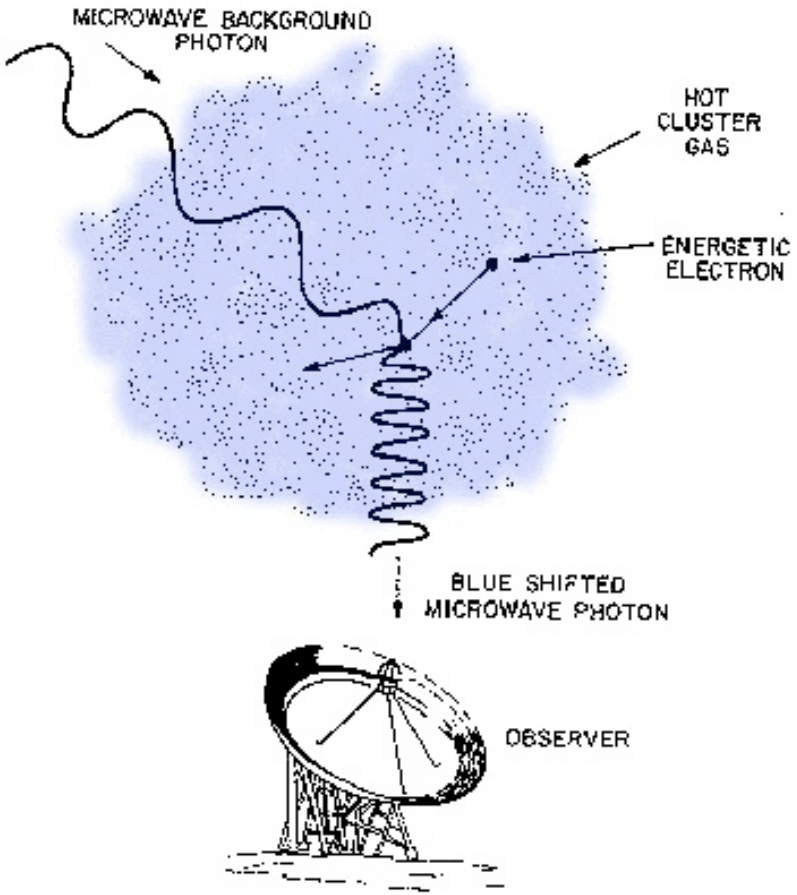

Sunyaev-Zeldovich

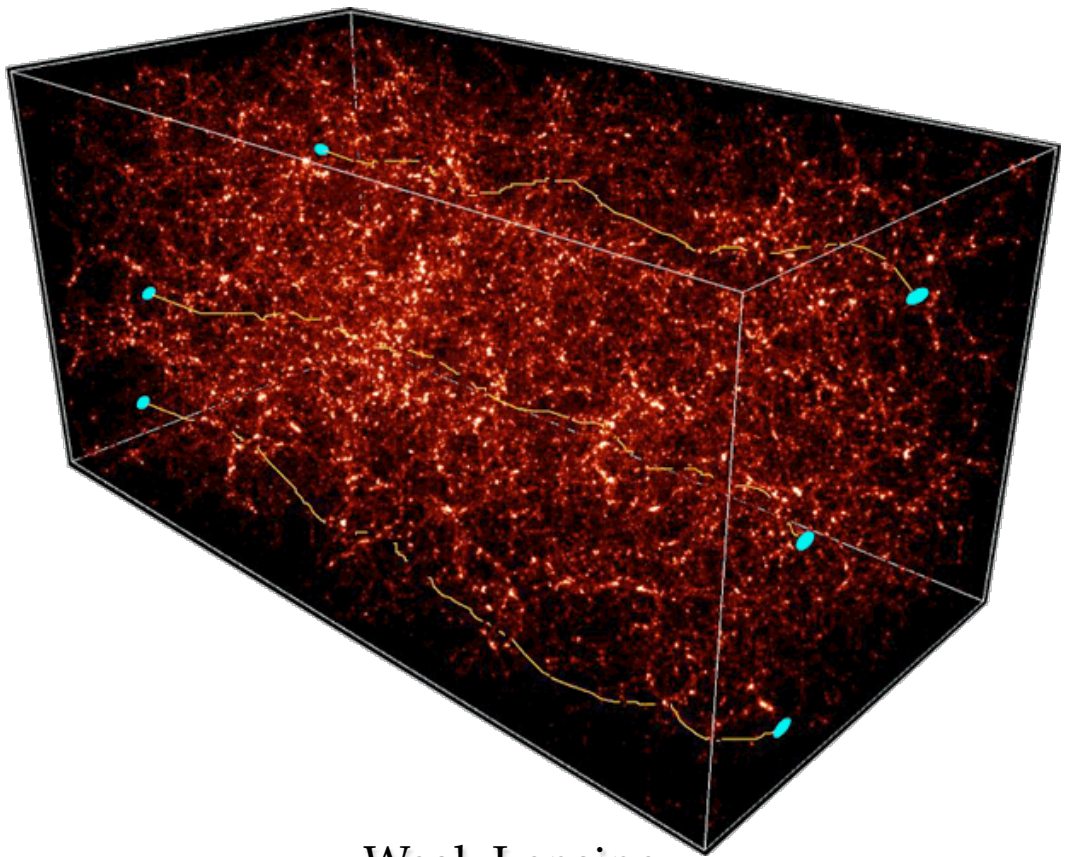

Weak Lensing

Sunyaev–Zel'dovich Effect

SZ effect arises due to inverse Compton scattering of CMB photons by hot electrons along the line of sight.

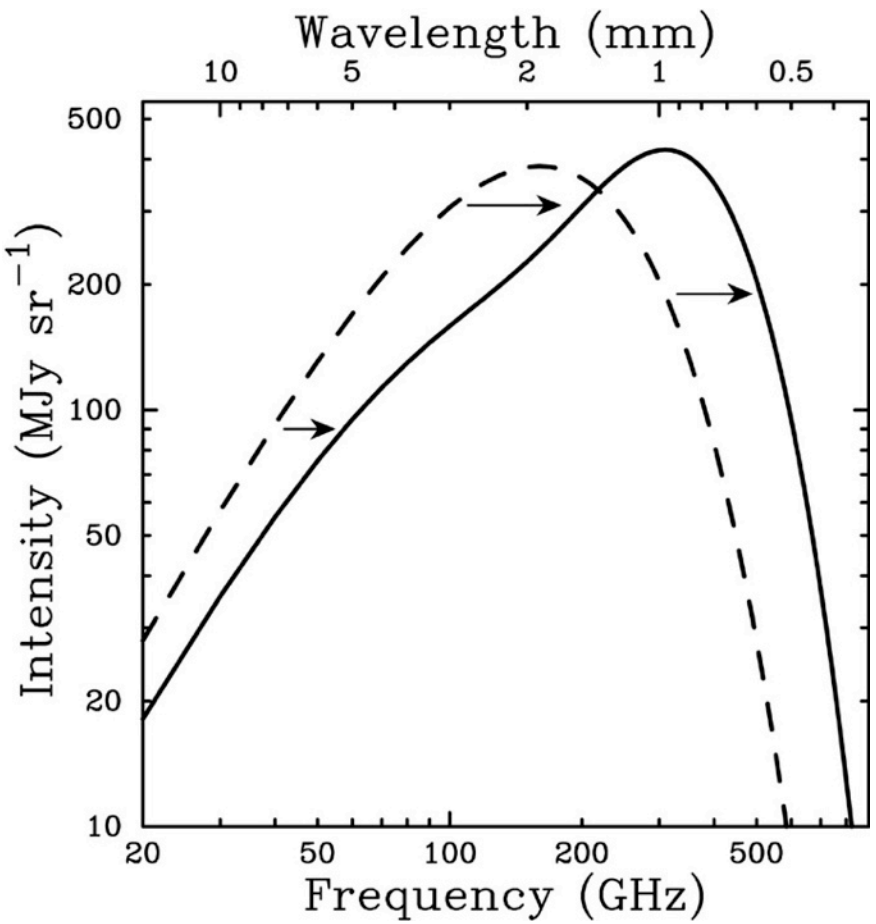

$$\Delta T_{SZ} / T_0 = y \cdot S_{SZ}(x) \;\rightarrow\; -2y \quad (x \ll 1)$$

$$S_{SZ}(x) = x\,coth(x/2) - 4 \qquad (x = h\nu/kT)$$

$$y = \int dl\, (k_B\, \sigma_T / m_e\, c^2)\, n_e T_e$$

Construction of Full-Sky SZ Map(s)

SZ map from linear combination of Planck frequency bands: ν_i = 100, 143, 217, 353 GHz.

$$T_{SZ}/T_0 \equiv y\, S_{SZ}(\nu_i) = \sum b_i\, T(\nu_i)$$

1. $\sum b_i\, S_{SZ}(\nu_i) = 1$ $\qquad S_{SZ}(x) = x\, coth(x/2) - 4 \;\; (x = h\nu/kT)$

2. $\sum b_i\, S_{CMB}(\nu_i) = 0$ $\qquad S_{CMB}(x) = 1$

3. $\sum b_i\, S_{"dust"}(\nu_i) = 0$ $\qquad S_{"dust"}(\nu_i) = \nu^{\beta}\, g(x)$

4. $\sum b_i\, S_{CO}(\nu_i) = 0$ *or* $\sum b_i\, S_{"radio"}(\nu_i) = 0$ (optional)

Planck Full-Sky Maps: ~~9~~ 4 Bands

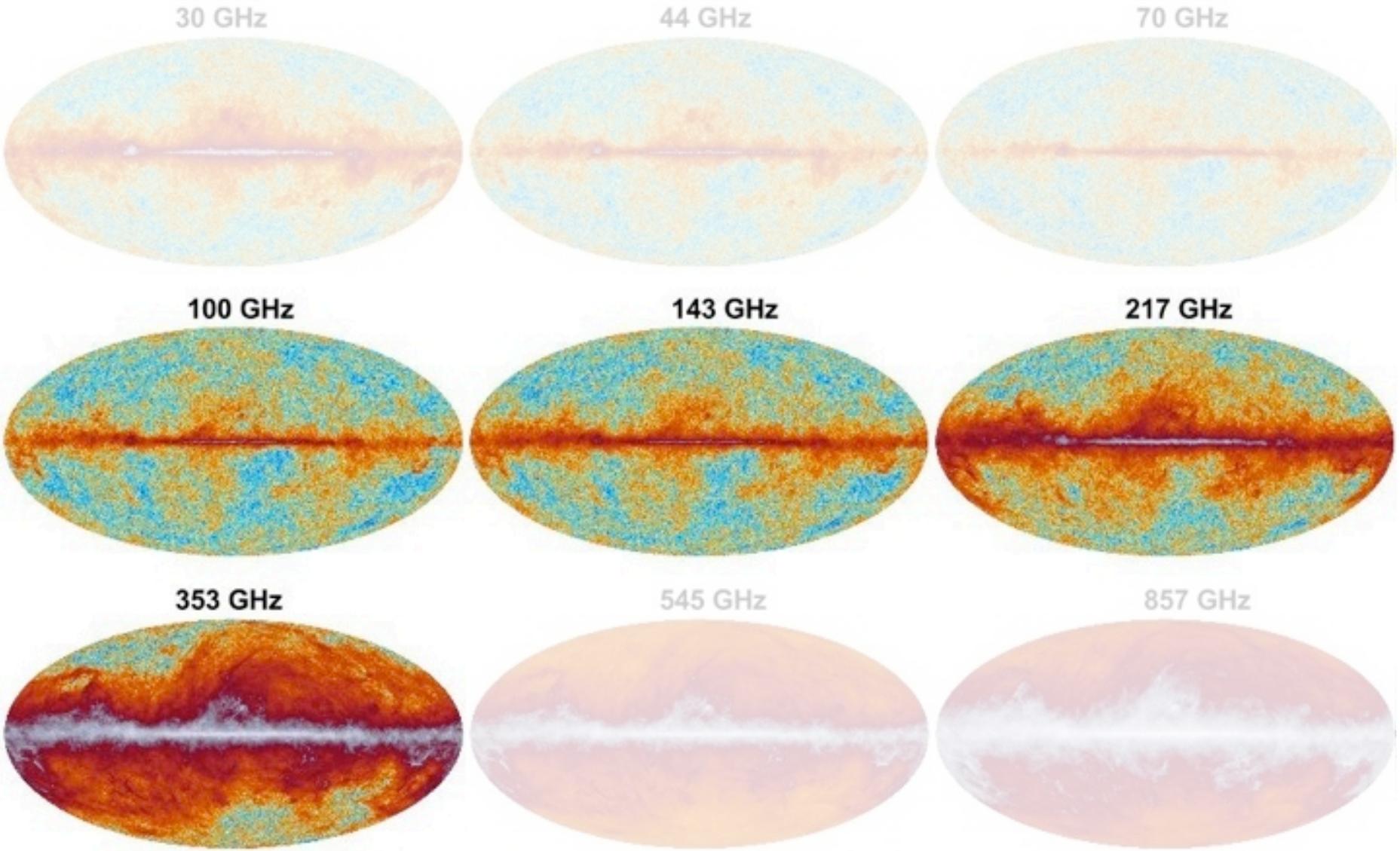

Planck SZ y map, version A

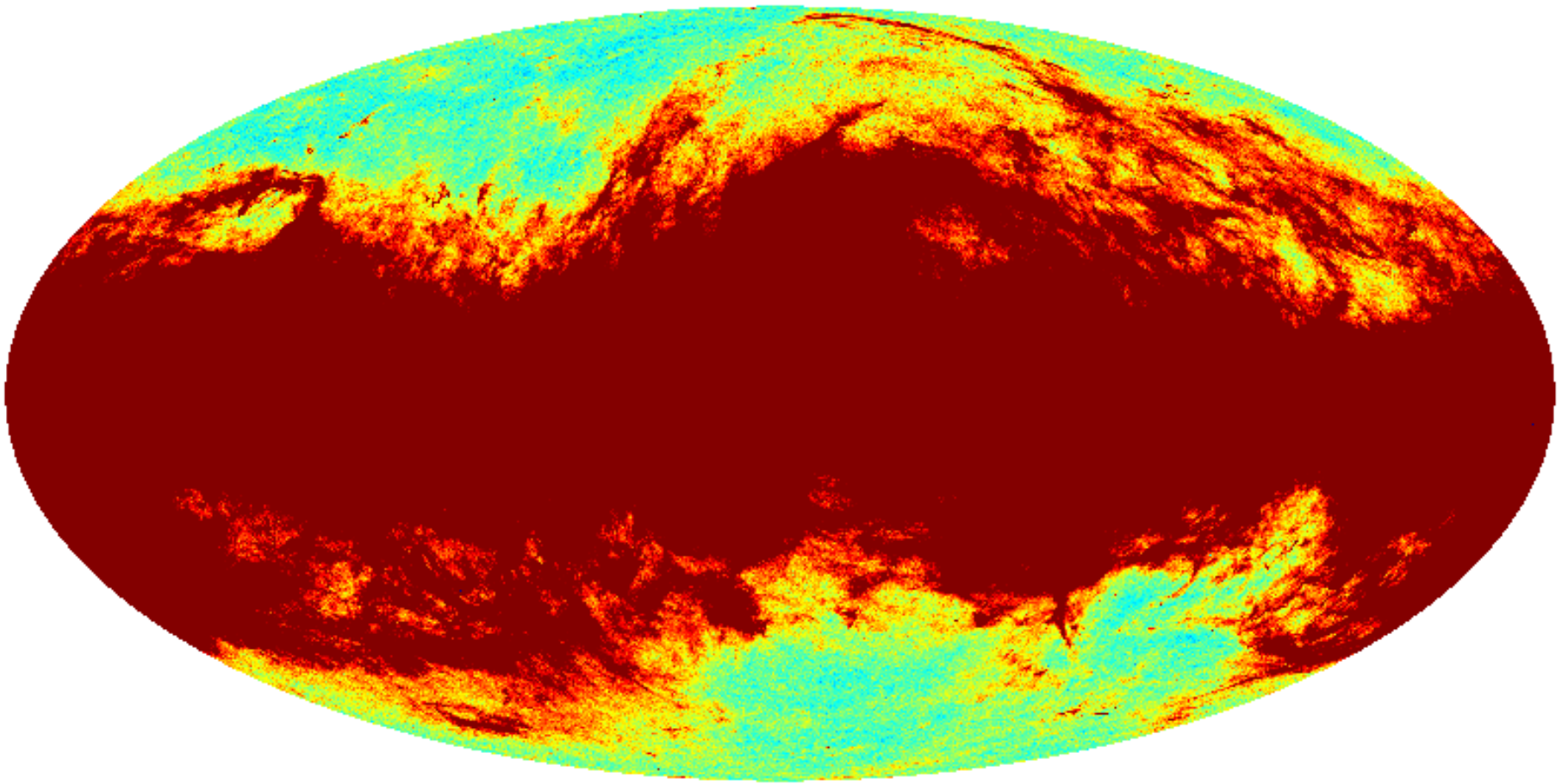

No dust rejection, $r_{2.0}(100\ \mathrm{GHz}) = 44$

Planck SZ y map, version E

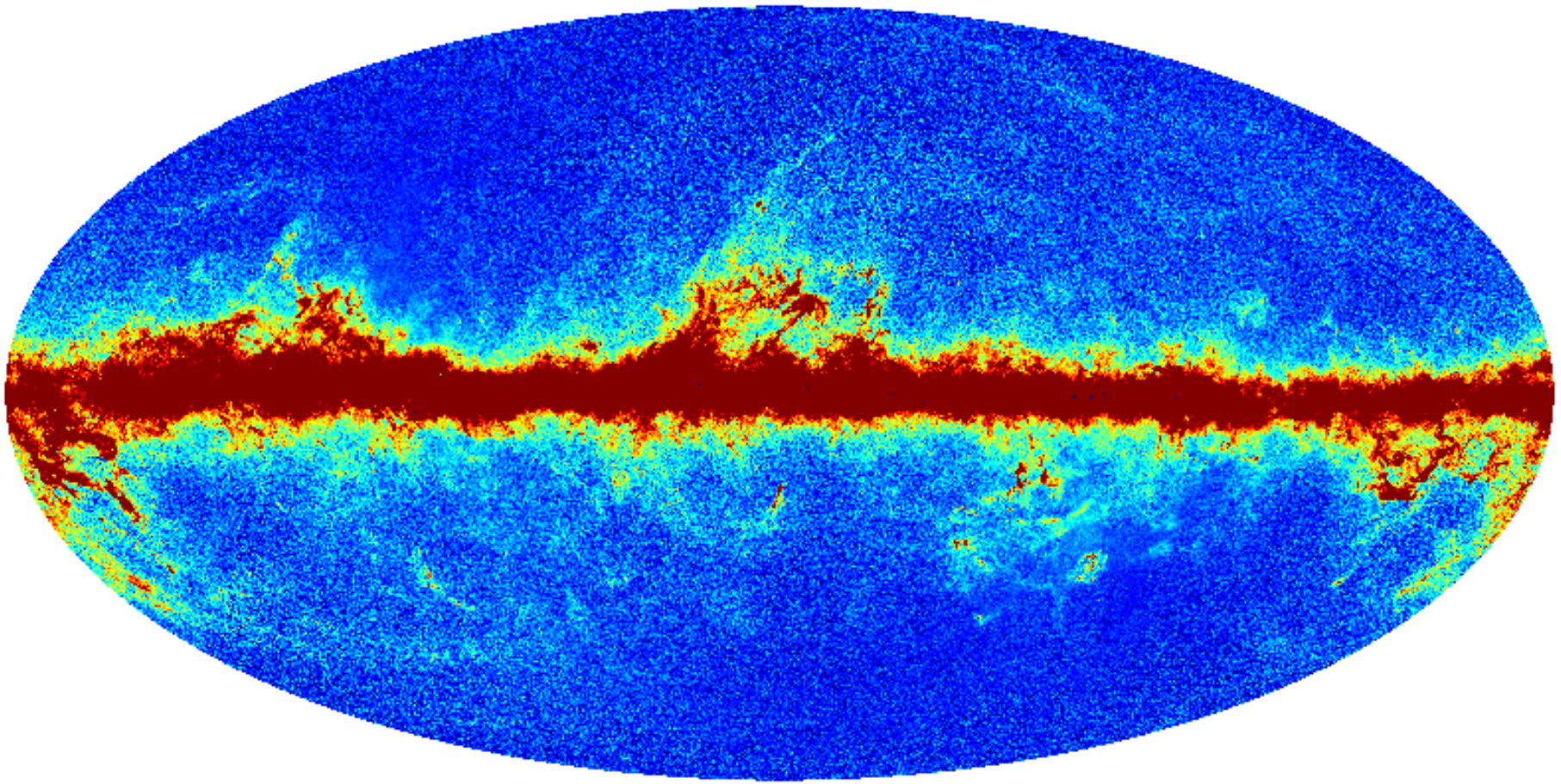

Reject $\beta_{\rm dust} = 2.0,\ \ r_{2.0}(100\ {\rm GHz}) = 0$

Planck SZ y map, version D

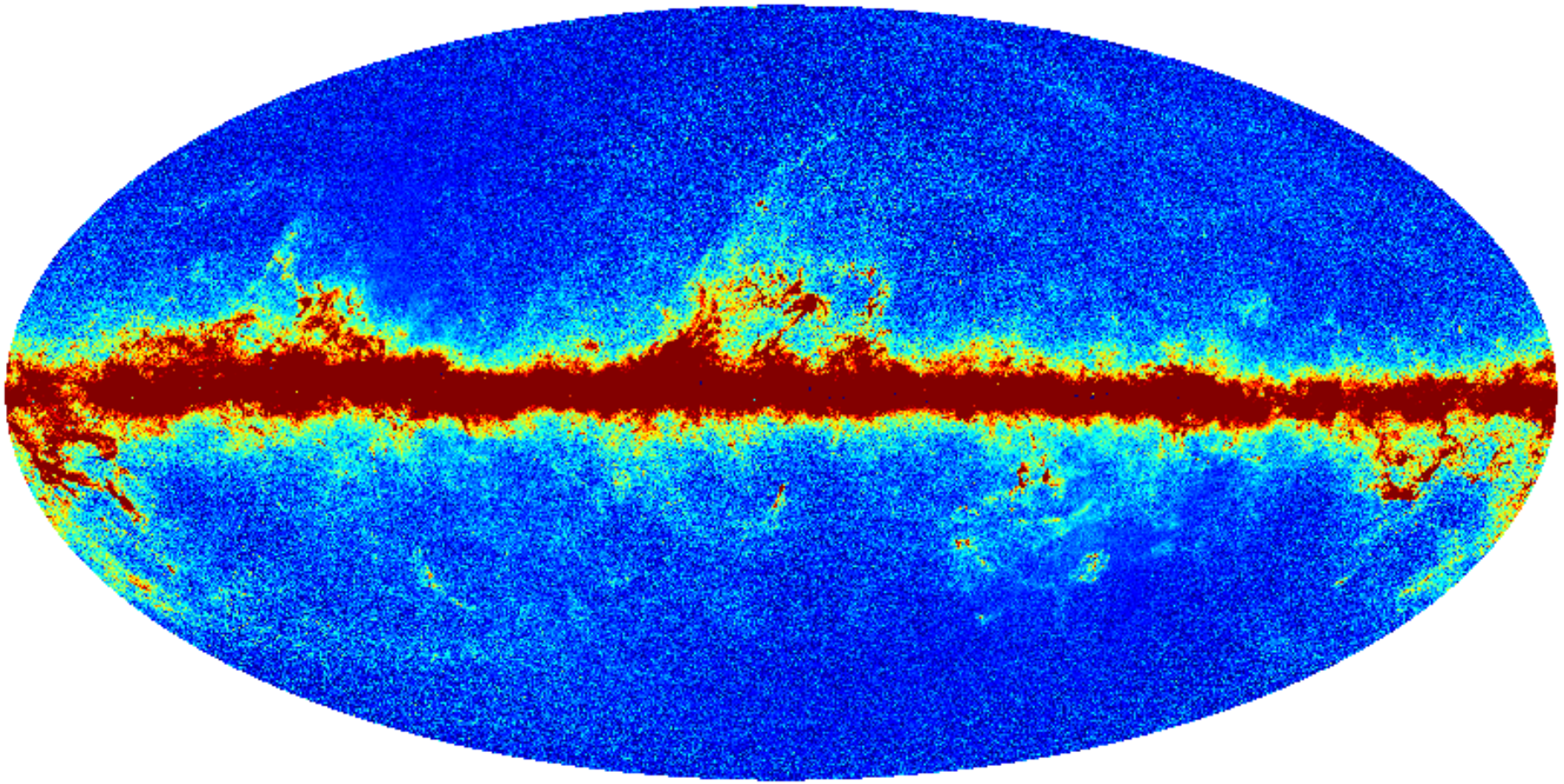

Reject $\beta_{\rm dust} = 1.8,\ \ r_{2.0}(100\ {\rm GHz}) = -0.9$

Planck SZ y map, version C

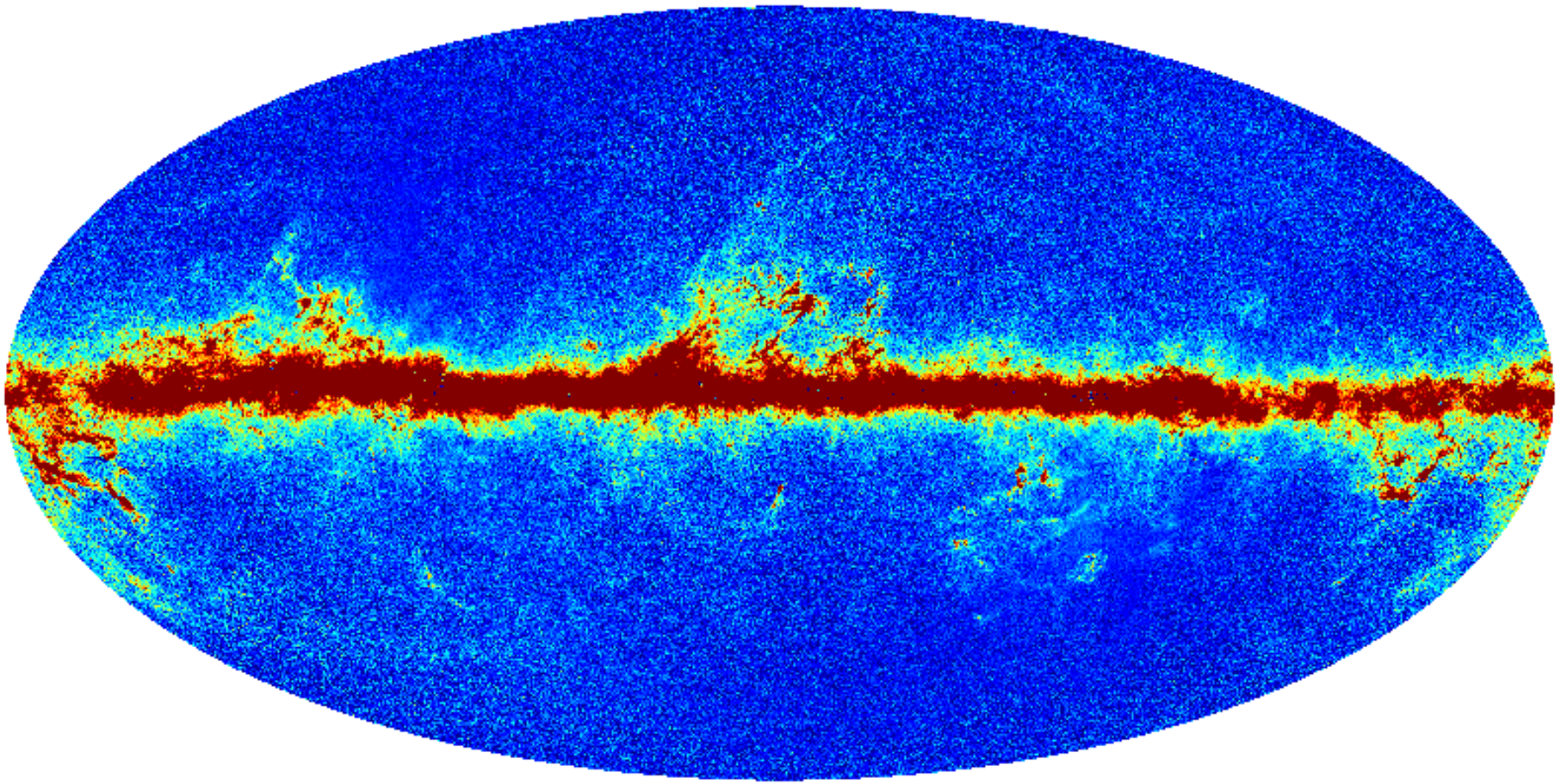

Reject $\beta_{\rm dust} = 1.6$, $r_{2.0}(100\ {\rm GHz}) = -2.0$

Planck SZ y map, version B

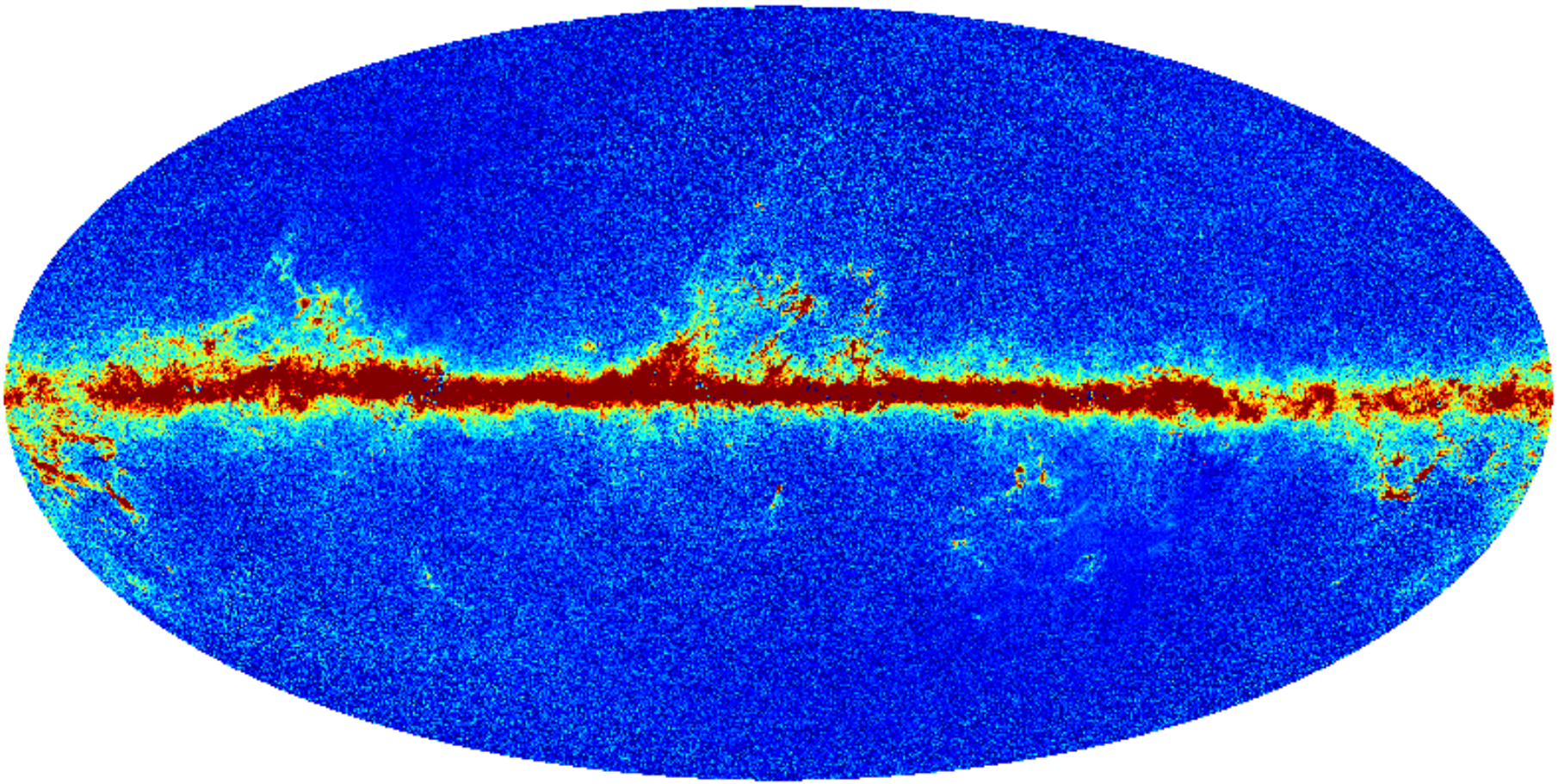

Reject $\beta_{\rm dust} = 1.4$, $r_{2.0}(100\ {\rm GHz}) = -3.1$

Planck SZ y map, version F

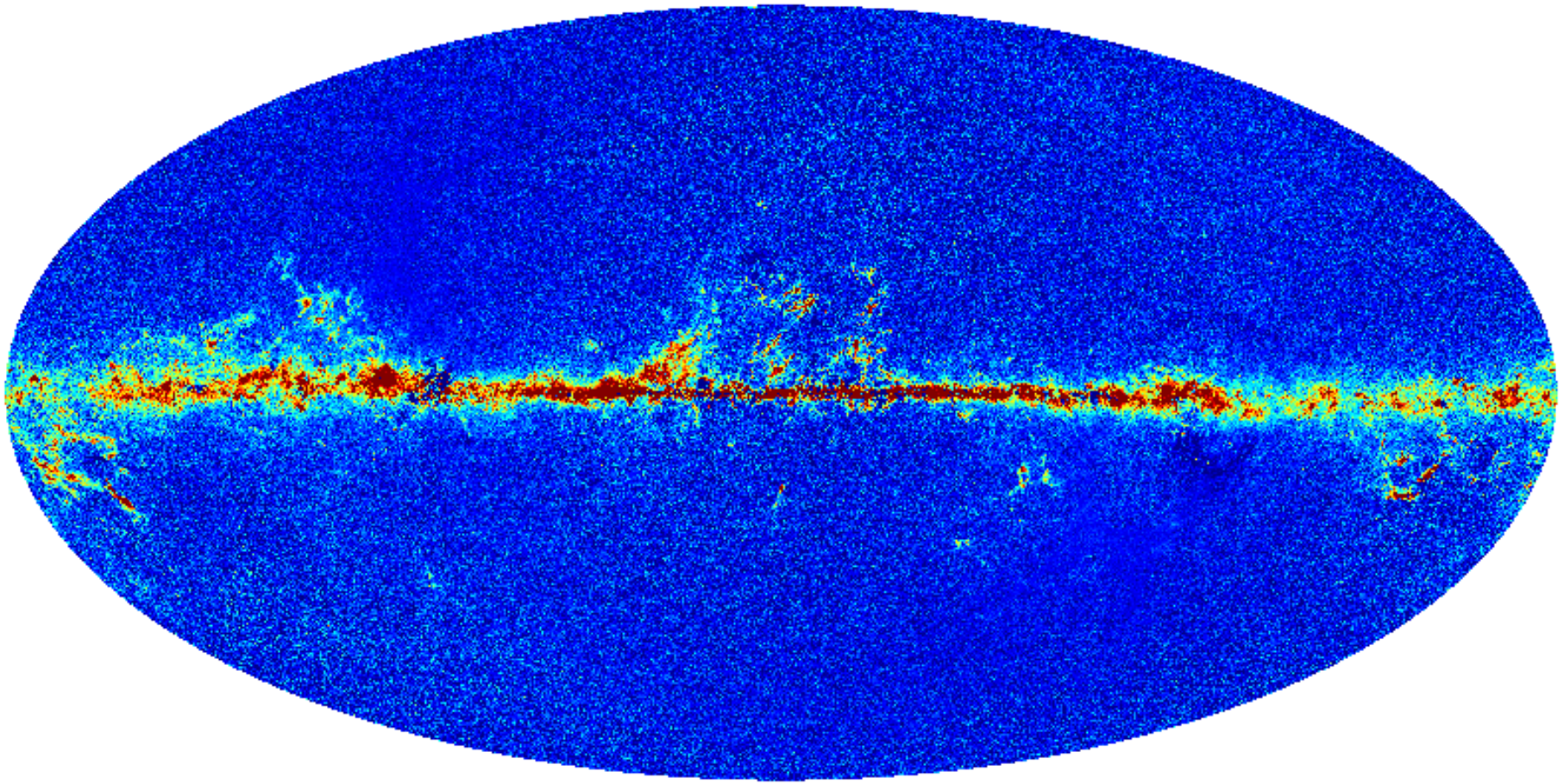

Reject $\beta_{\rm dust} = 1.2,\ \ r_{2.0}(100\ {\rm GHz}) = -4.4$

Planck SZ y map, version G

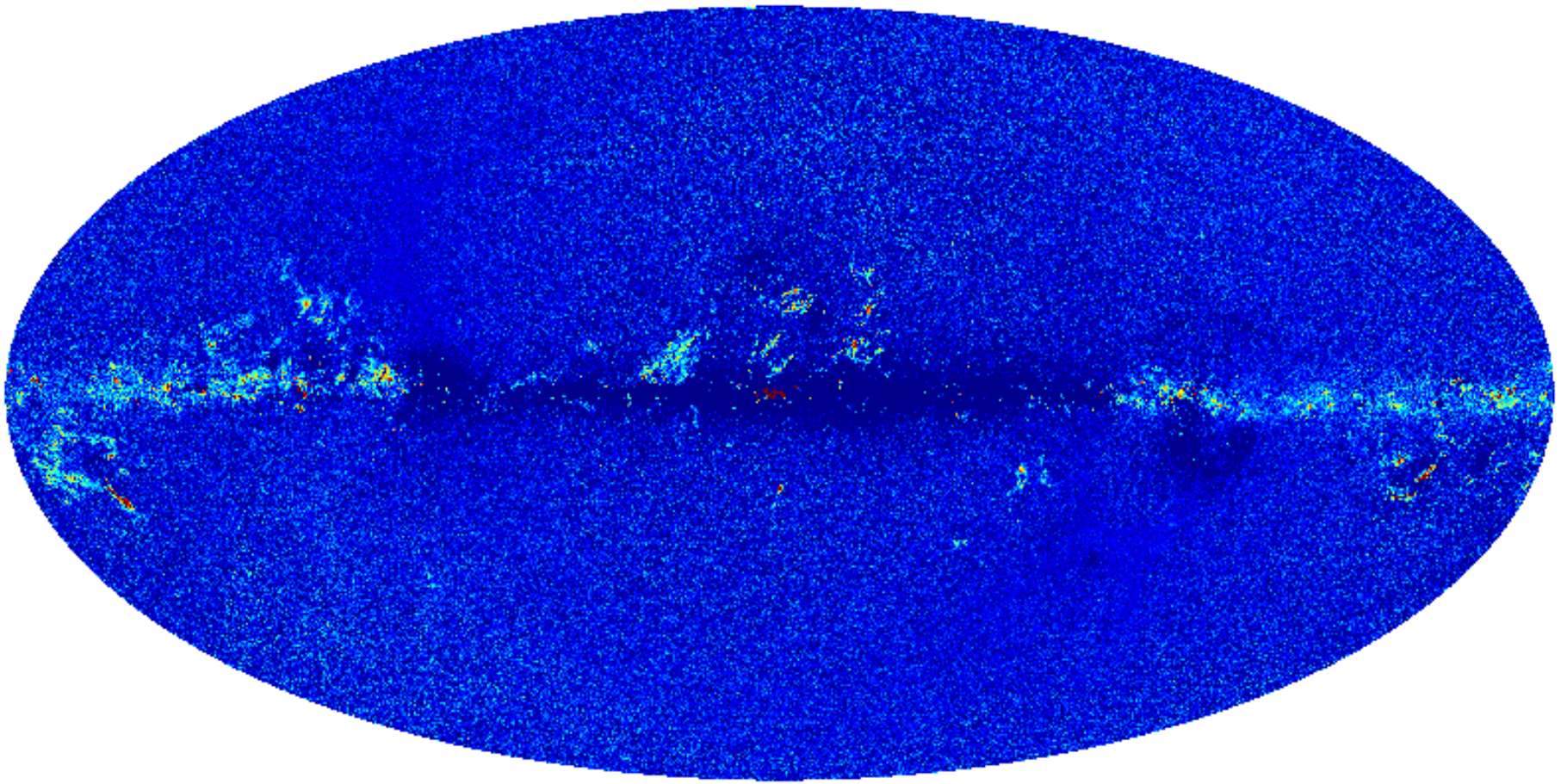

Reject $\beta_{\rm dust} = 1.0,\ \ r_{2.0}(100\ {\rm GHz}) = -5.7$

Planck SZ no-y map, version E

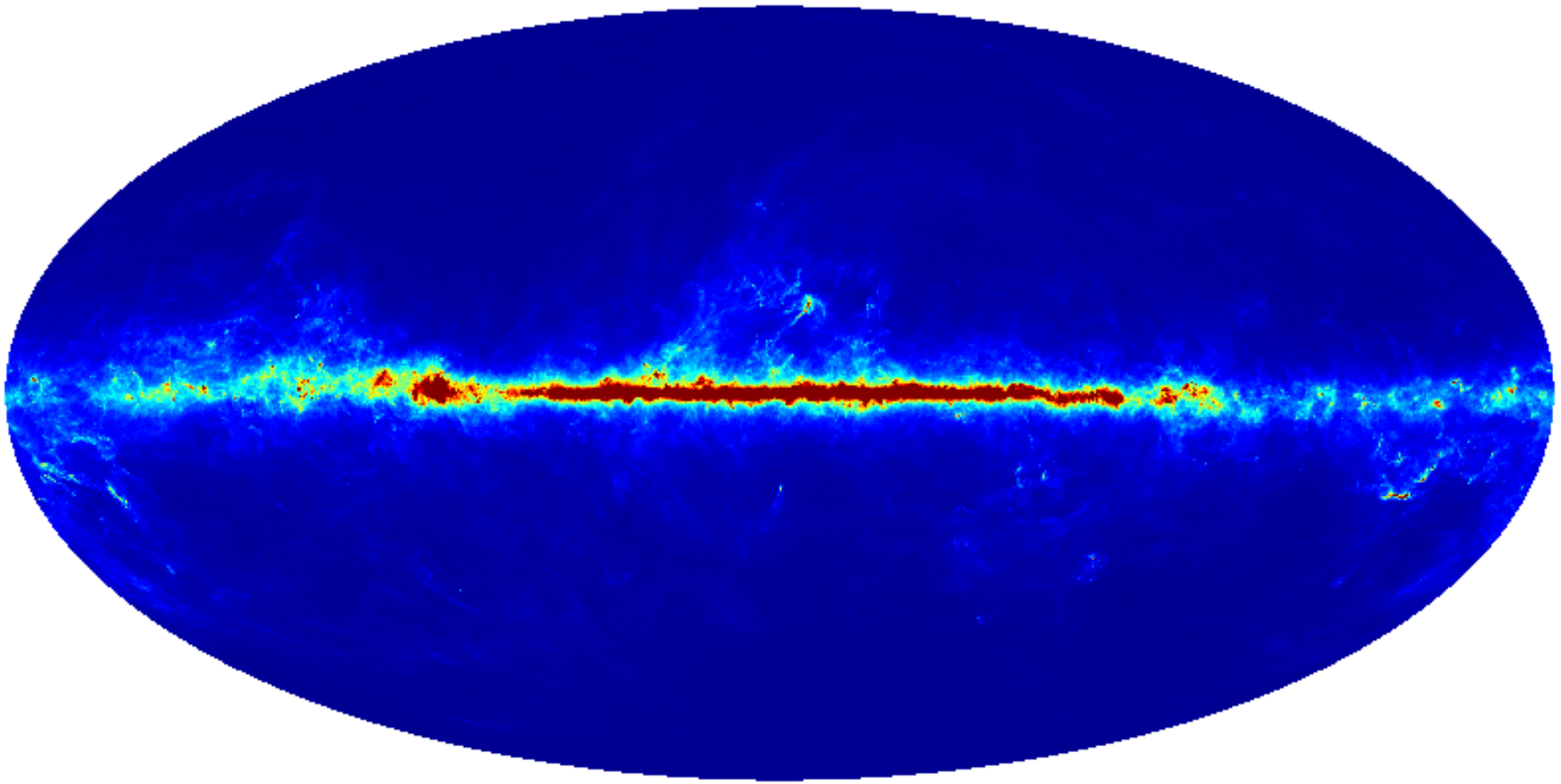

Reject $S_{SZ}(\nu)$, retain $\beta_{dust} = 1.8$

Planck y in Cross Correlation with other tracers

Dark Matter Map (κ) from CFHT Lensing

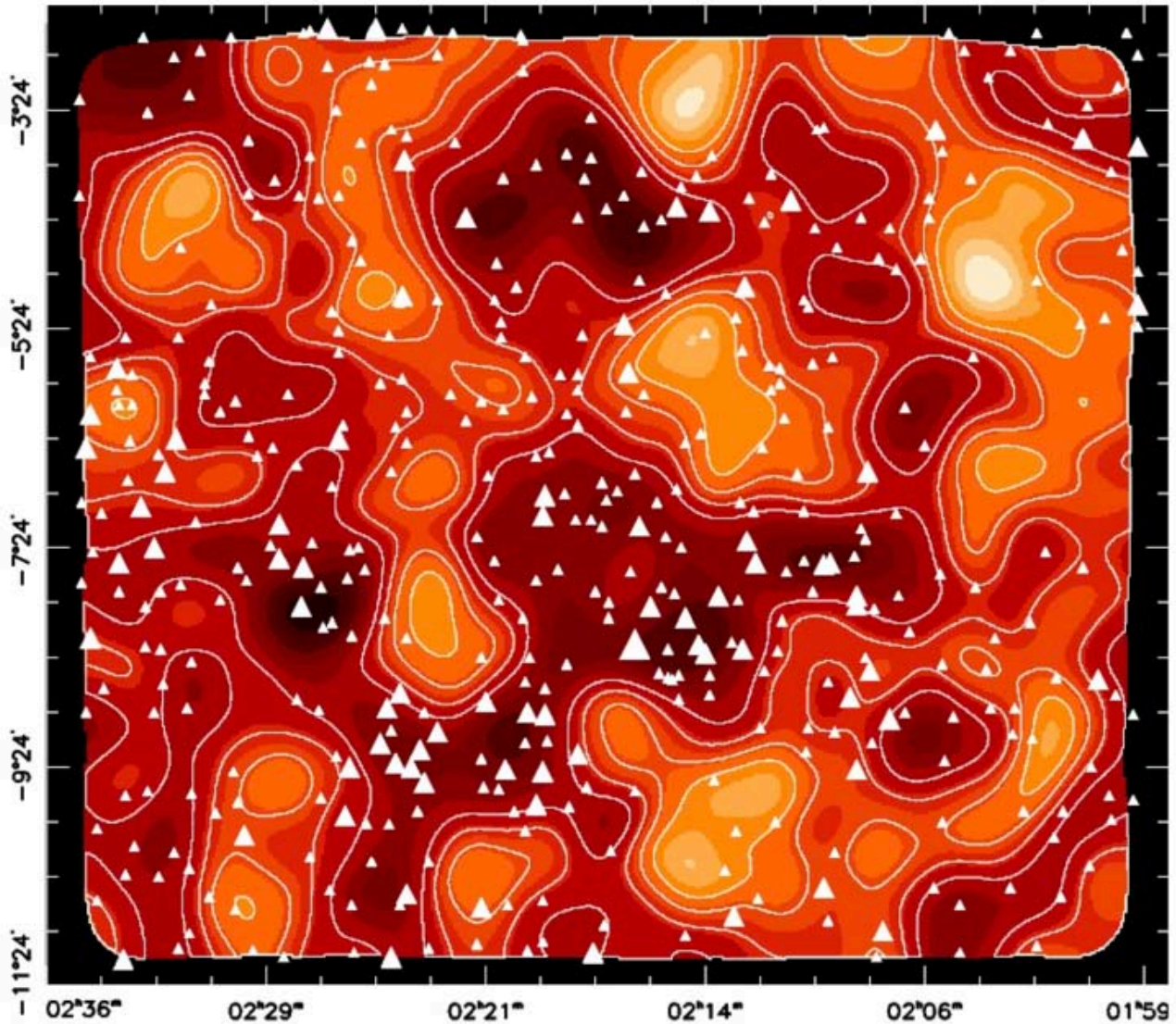

Projected mass map, κ, from CFHTLens, triangles indicate troughs in galaxy density.

Cross Correlation: y × κ

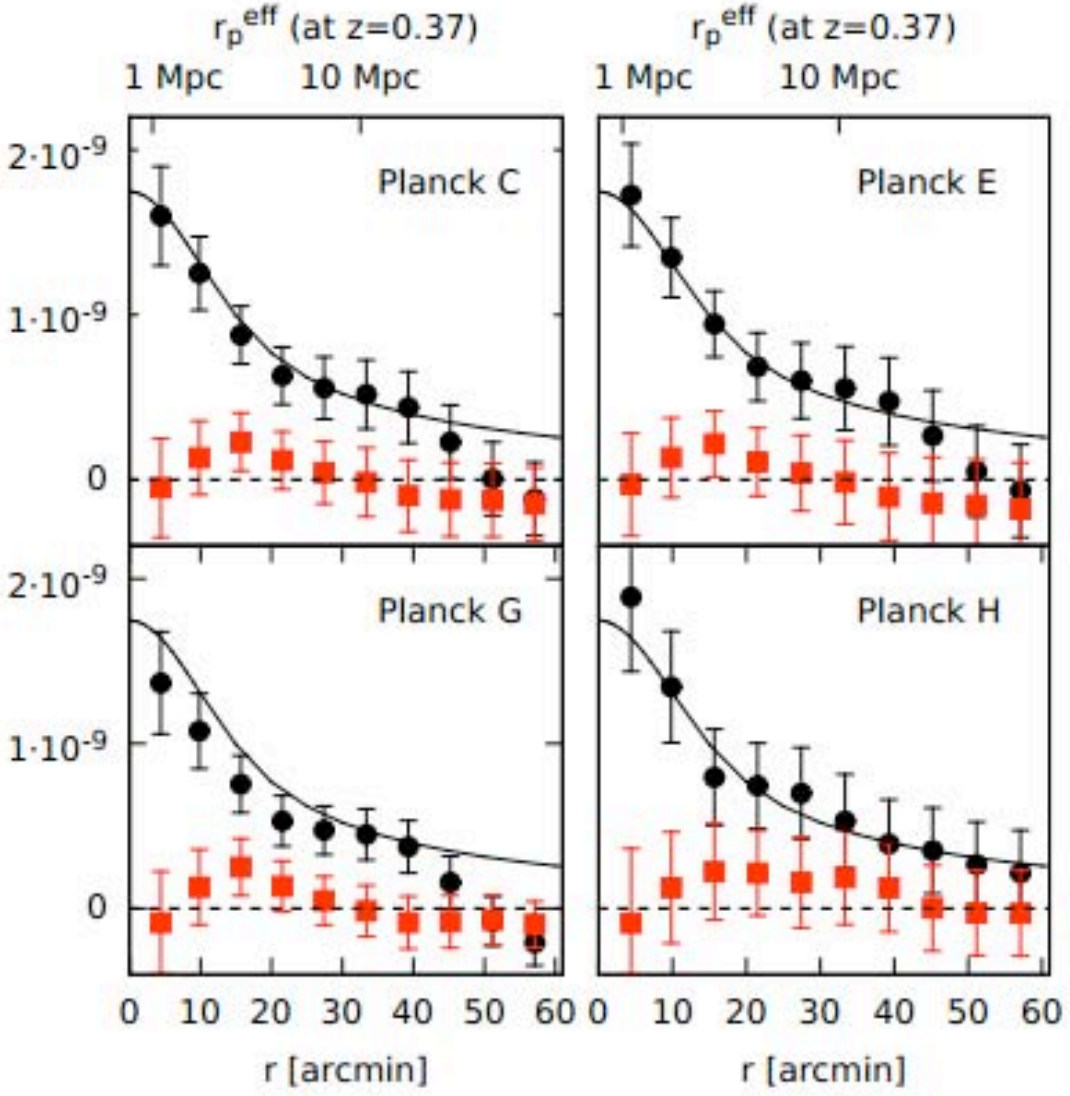

van Waerbake, Hinshaw, Murray; arXiv:1310.5721

Significant detection of ionized gas spatially correlated with dark matter.

Different panels show correlations with different y maps to test for galactic contamination.

Amplitude constrains the product:

$$n_e \cdot T \cdot b$$

n_e = electron density
T = gas temperature
b = gas bias

y × κ, Quality Tests

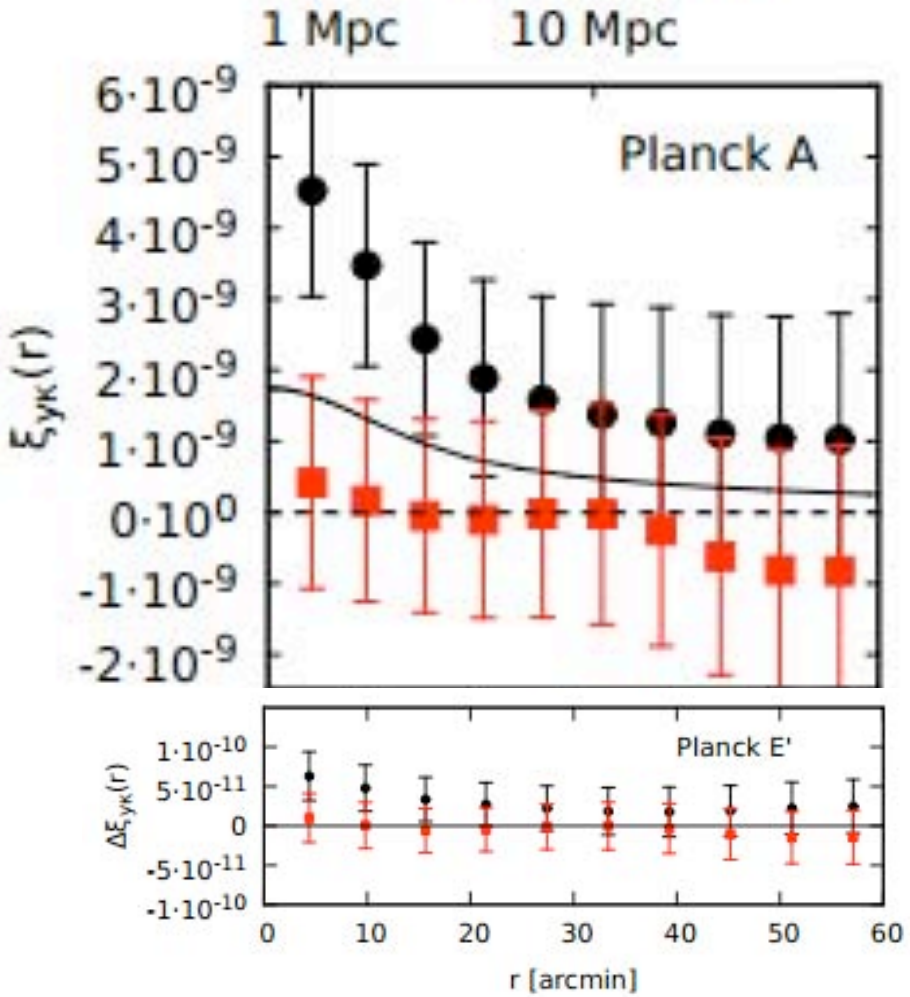

Top panel show result with no attempt to cancel galactic emission. Cosmic signal persists.

Bottom panel shows a null test: cross correlation with y map that should be zero.

Final measurement:

$$\left(\frac{b_{\rm gas}}{1}\right)\left(\frac{T_e(0)}{0.1\ {\rm keV}}\right)\left(\frac{\bar{n}_e}{1\ {\rm m}^{-3}}\right) = 2.01 \pm 0.31 \pm 0.21,$$

y × κ, Astrophysical Modeling

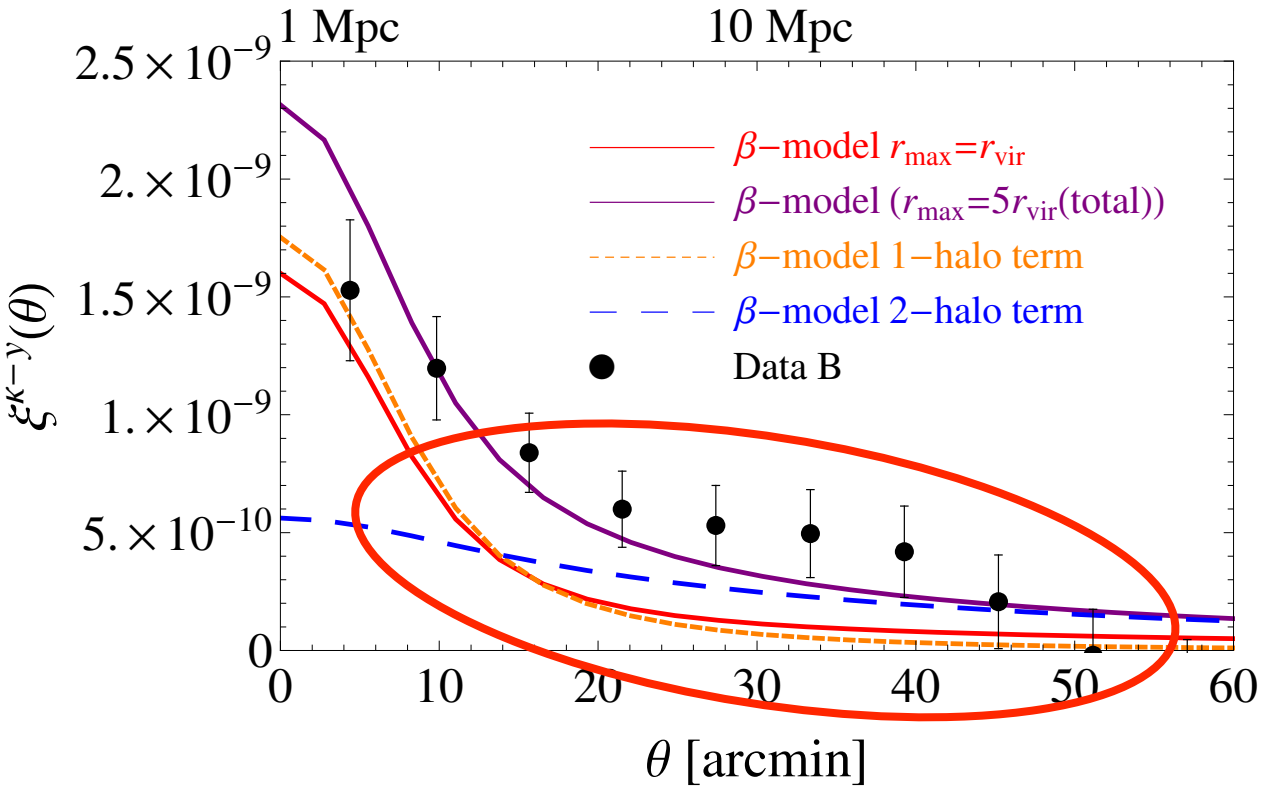

Signal persists to separations of 10's of Mpc.

Ma et al. fits a halo model to the observed correlation function. A β model fits well, but in this context the data requires a 2-halo term to fit the large angular scale separation.

Ma et al, arXiv:1404.4808

Cross Correlation with SDSS LRGs

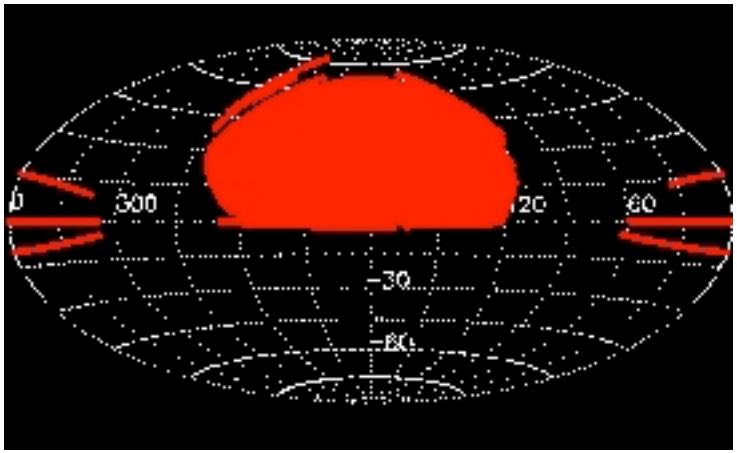

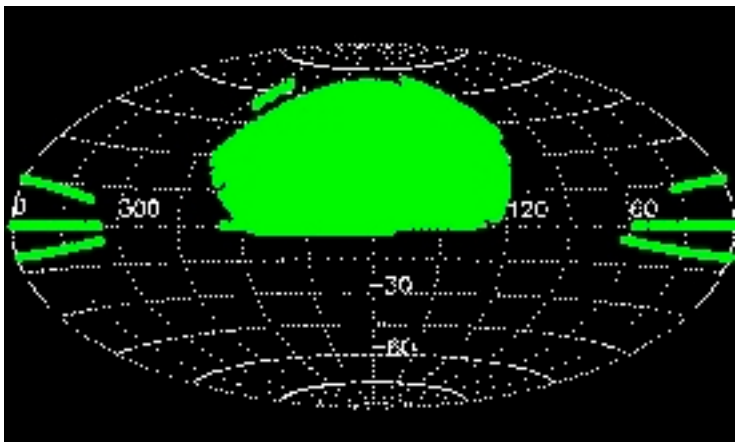

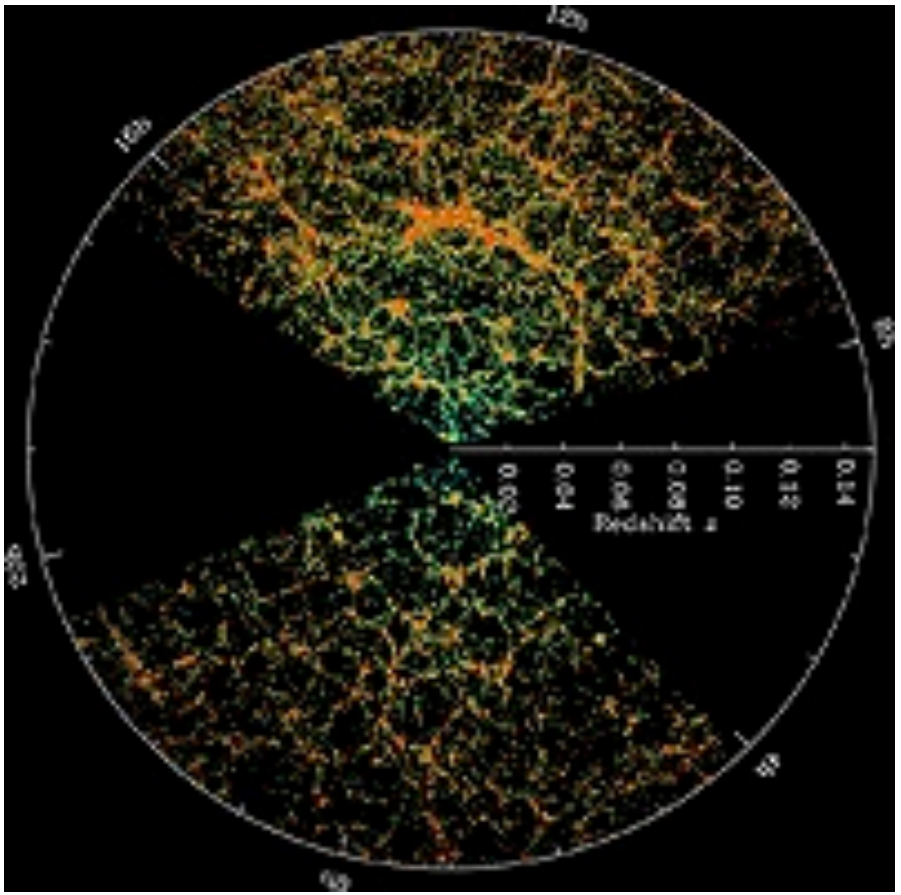

SDSS DR7 sky coverage

SDSS LRG Pairs in Weak Lensing

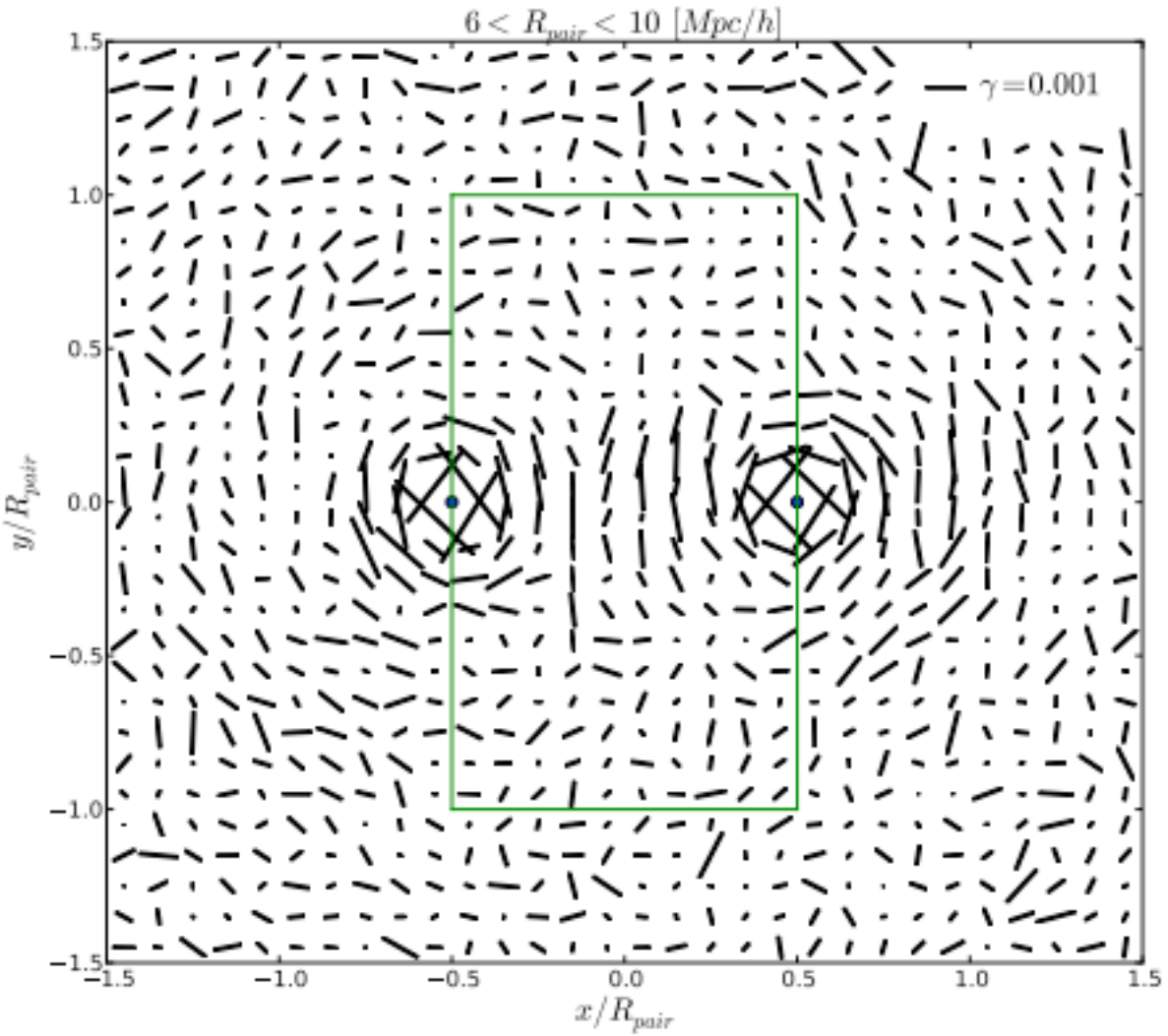

Kazin et al produced an LRG pair catalogue from 110,000 LRGs producing ~220,000 pairs with

6 Mpc < r < 18 Mpc

Clampitt et al analyzed WL shear in vicinity of pairs and claim evidence for dark matter filaments connecting the objects.

Left - shear stacked on LRG pairs, prior to circular halo correction.

Clampitt, Jain, Takada, arXiv:1402.3302

Planck y at SDSS LRG Pairs

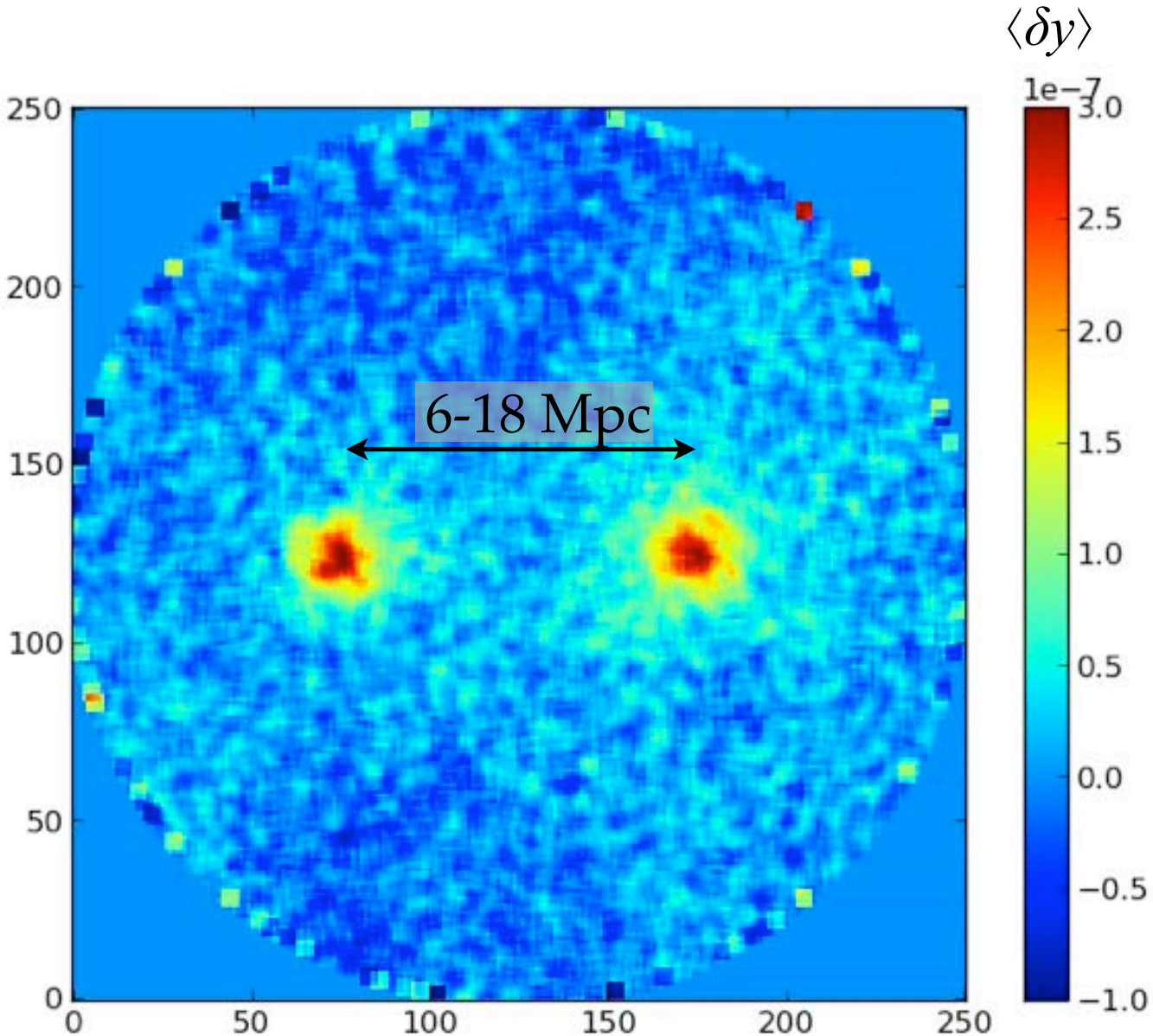

Preliminary -

Planck y map stacked on the normalized SDSS LRG pair catalogue, 220,000 pairs with:

6 Mpc $< r_\perp <$ 18 Mpc

Question: is there evidence for a gas filament bridging the pairs?

Not obviously...

Planck Pair Stack – Randomized

Preliminary - to remove spherical (circular) contribution due to each LRG, perform the stack with a random orientation of y map relative to line joining the pair.

$\langle \delta y \rangle$

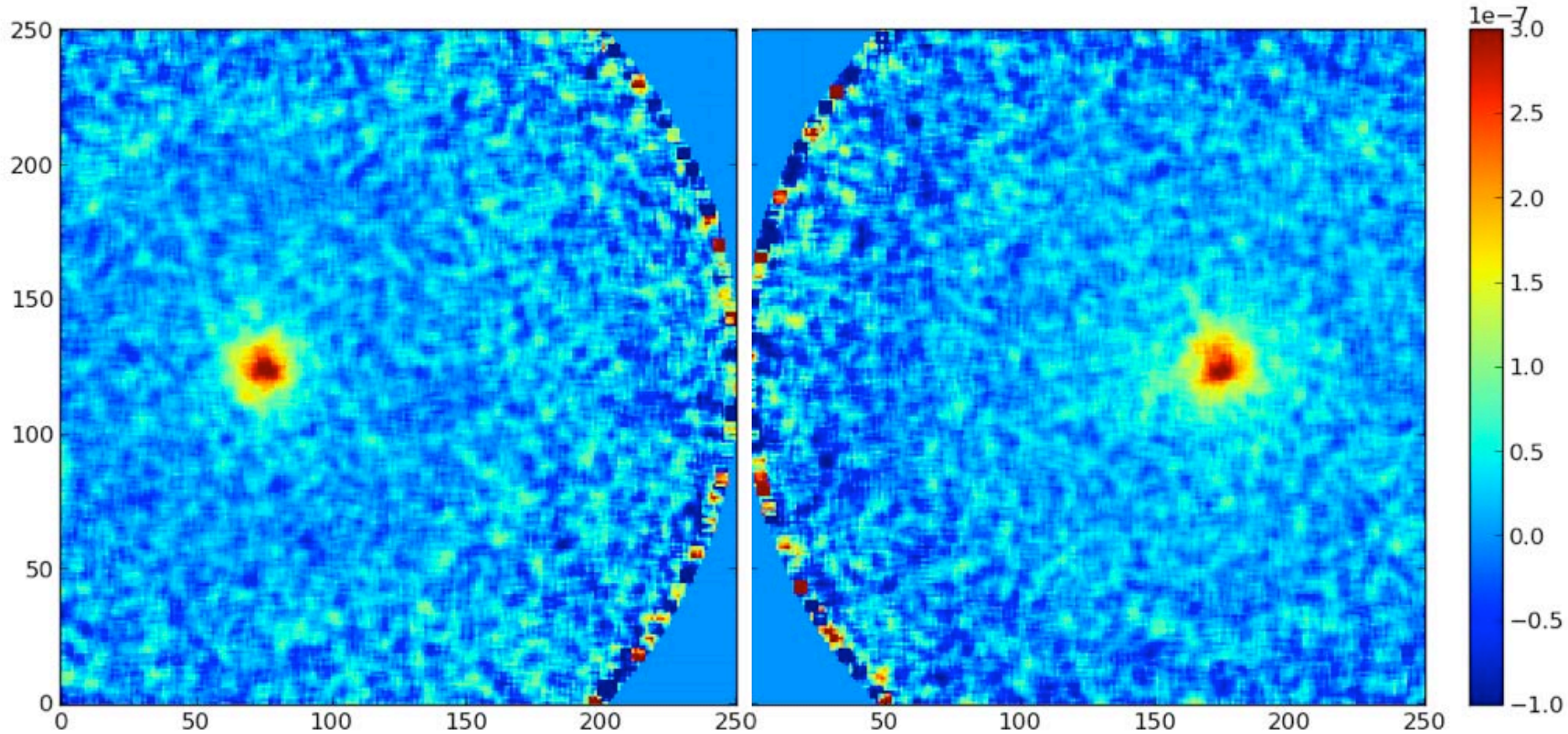

Residual y Map After Source Subtraction

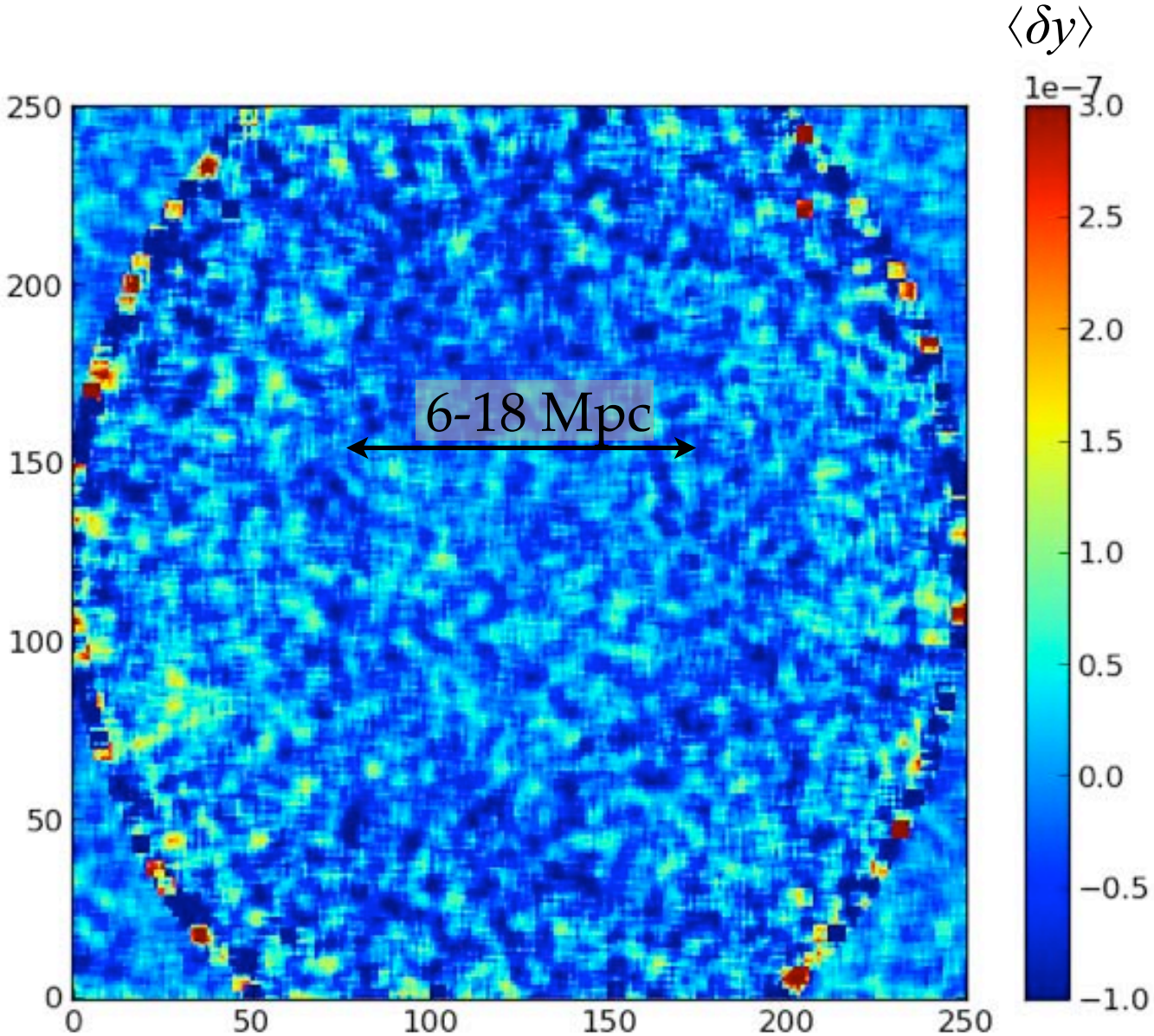

Preliminary -

After removing contribution from circularized LRG gas, there is is no significant signal remaining.

Planck y at SDSS LRG Pairs

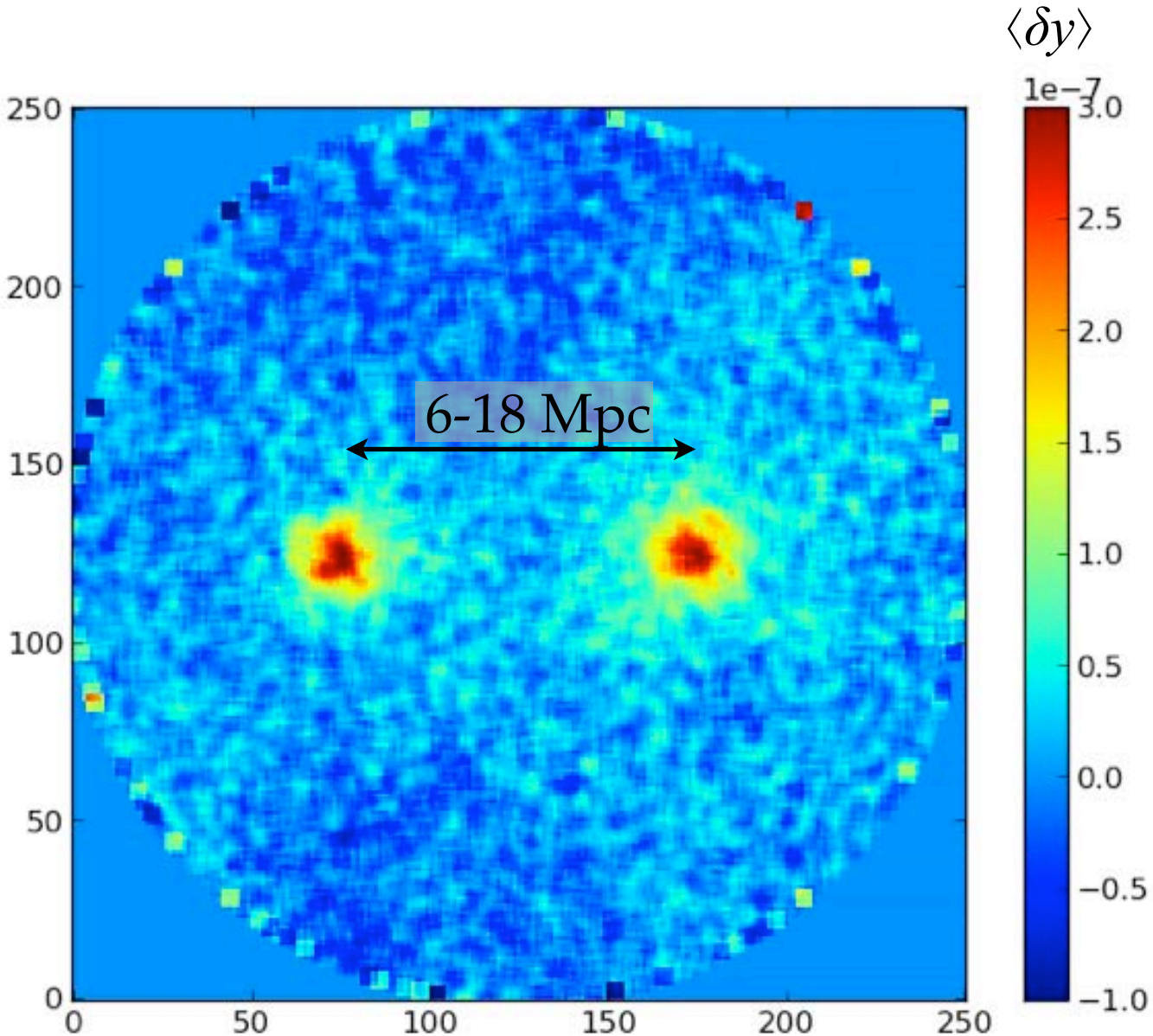

Preliminary -

Planck y map stacked on the normalized SDSS LRG pair catalogue, 220,000 pairs with:

6 Mpc $< r_\perp <$ 18 Mpc

Question: is there evidence for a gas filament bridging the pairs?

Not obviously...

Planck y at SDSS LRG Pairs

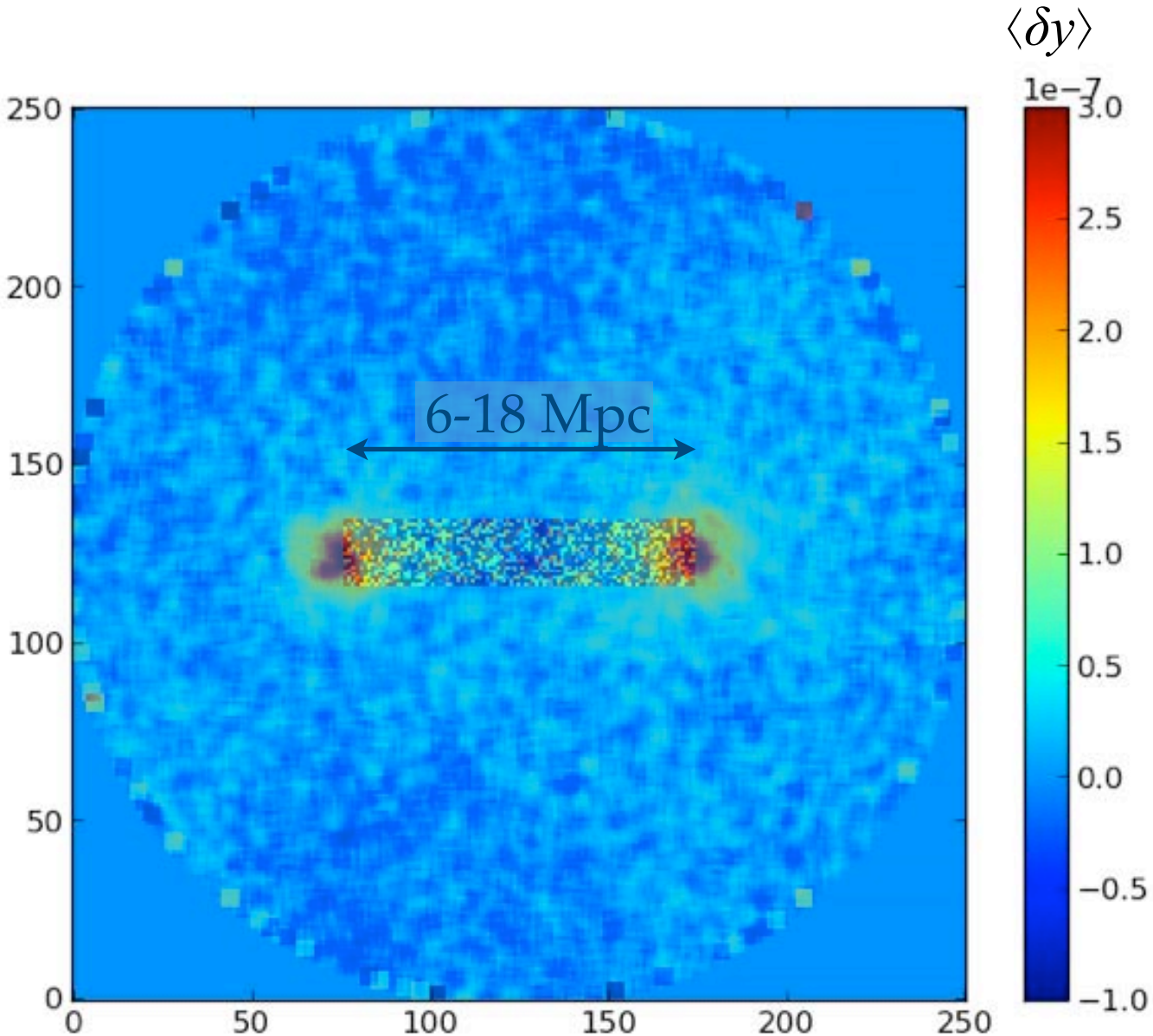

After circular halo subtraction, no significant signal left in the bridge region, as shown:

$\langle \delta y \rangle < 1.2 \times 10^{-8}$ (95% CL)

Planck y Summary

We create a set of full-sky Planck SZ y maps using linear combinations of 100, 143, 217, and 353 GHz data, with a range of residual foreground contamination.

We probe gas in cross correlation with CFHTLens lensing mass maps and SDSS LRG pair catalogue to probe gas distributions that are difficult to trace.

Significant correlation is seen with lensing mass. Data is reasonably well fit by a halo model, but requires gas out to $5 \times r_{\rm vir}$.

Clampitt et al analyzed WL shear in vicinity of pairs and claim evidence for dark matter filaments connecting the objects. We stack Planck y on the same sample and find no evidence for a "gas bridge" at the level of $y = 1.2 \times 10^{-8}$ (95% CL).

Galactic Foregrounds – 21 cm

Hydrogen Intensity Signal – Simulation

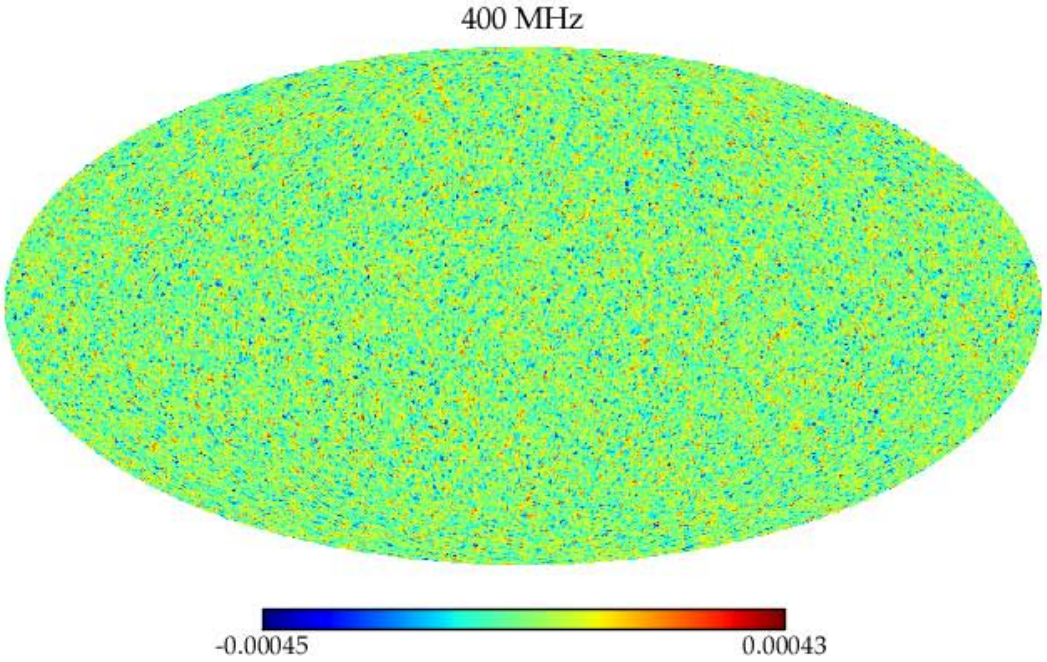

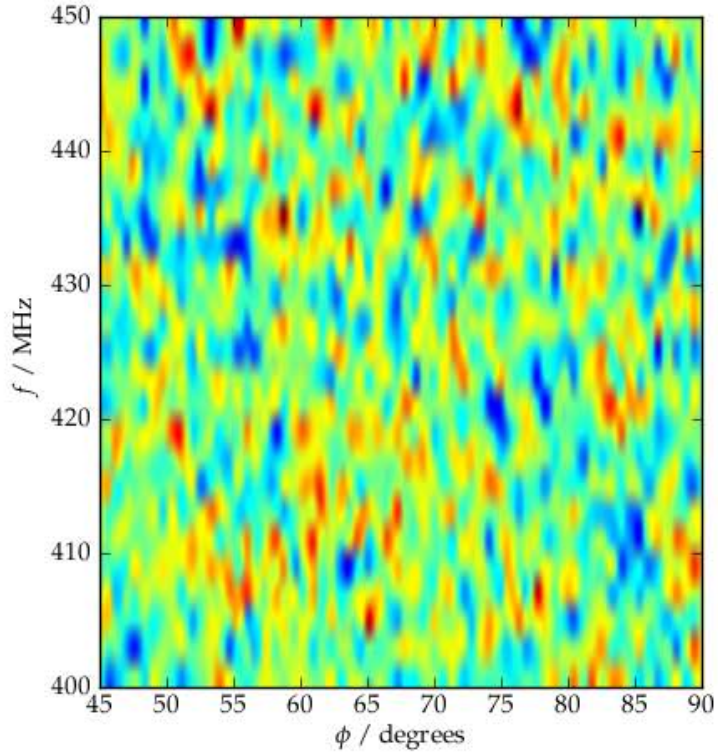

Simulated 21 cm signal, tracer of $\rho_{HI}(\theta,\varphi;z)$: $\Delta T \sim 1$ mK

left - over full sky at 400 MHz,

right - over 50 MHz at 1 declination

Main goal is to measure BAO structure in $P_{HI}(k)$, less concerned about amplitude of $P_{HI}(k)$.

Synchrotron Signal – Ideal Simulation

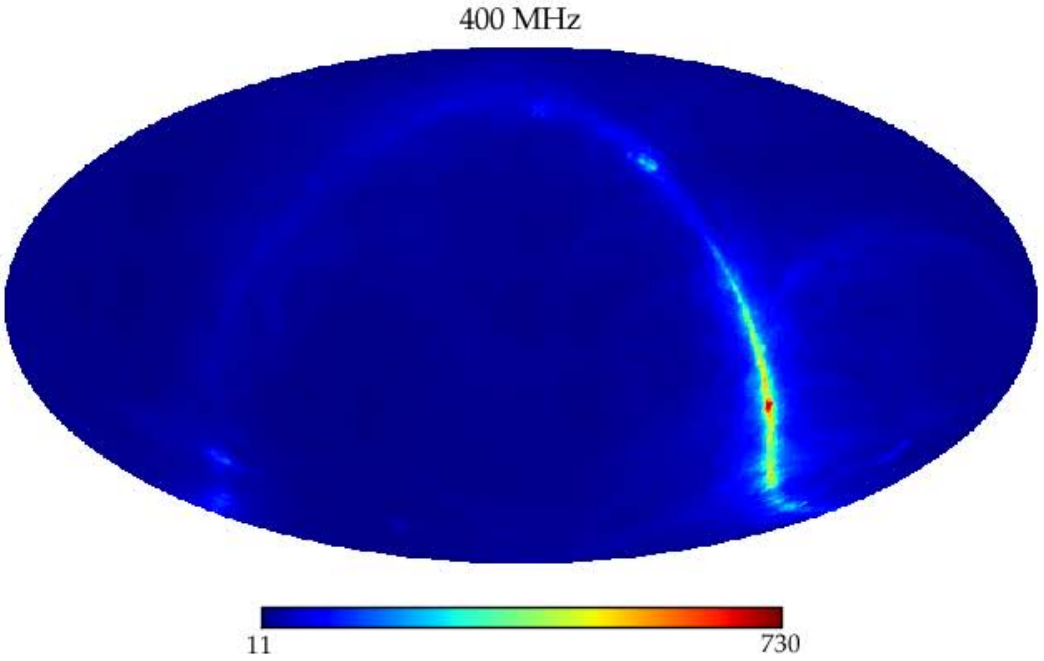

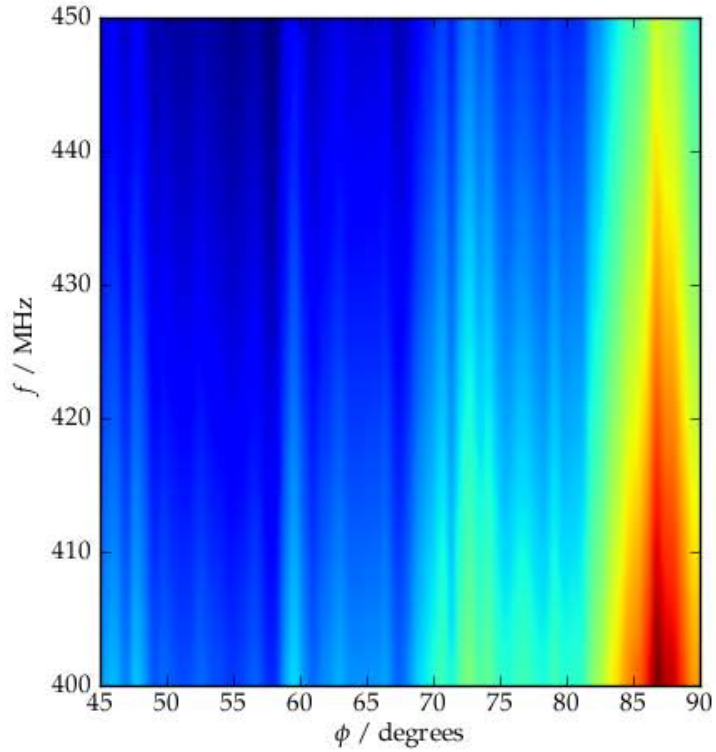

Modeled Galaxy signal, $\Delta T \sim 700$ K!

left - over full sky at 400 MHz,

right - over 50 MHz at 1 declination - spectrally smooth

Synchrotron Signal – Realistic Simulation

Ideal foreground:

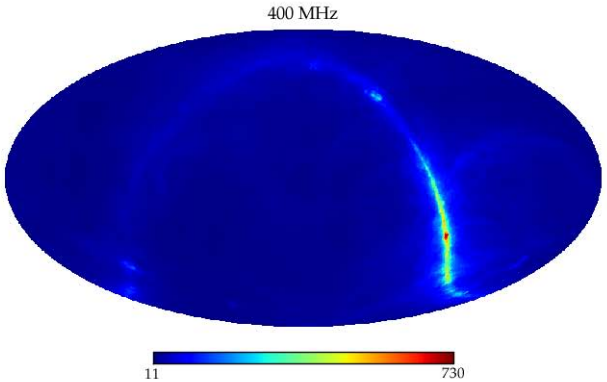

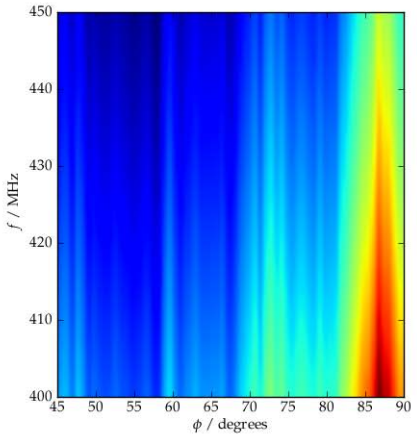

Observed foreground with beam response:

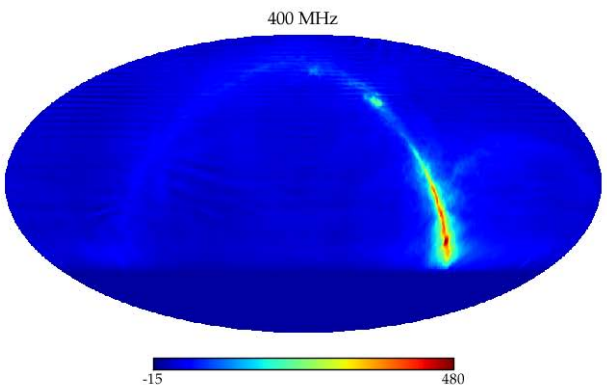

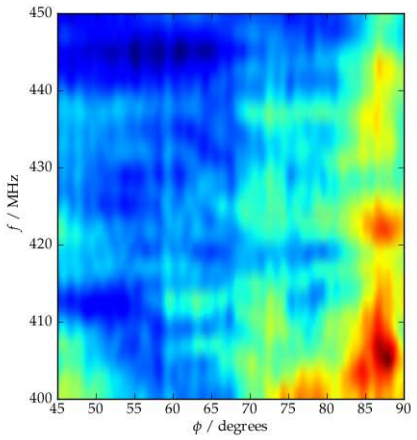

Foreground rejection must account for variable beam width , Faraday rotation and other effects. Beam calibration is critical, the Galt Telescope is critical!

The End